PHYSICAL REVIEW D **83,** 054020 (2011)

Light cone sum rules for the $\pi^0\gamma^*\gamma$ form factor revisited

S. S. Agaev,[1,2] V. M. Braun,[1] N. Offen,[1] and F. A. Porkert[1]

[1]*Institut für Theoretische Physik, Universität Regensburg, D-93040 Regensburg, Germany*

[2]*Institute for Physical Problems, Baku State University, Az–1148 Baku, Azerbaijan*

(Received 22 December 2010; published 14 March 2011)

We provide a theoretical update of the calculations of the $\pi^0\gamma^*\gamma$ form factor in the light cone sum rules framework, including up to six polynomials in the conformal expansion of the pion distribution amplitude and taking into account twist-six corrections related to the photon emission at large distances. The results are compared with the calculations of the $B \to \pi\ell\nu$ decay and pion electromagnetic form factors in the same framework. Our conclusion is that the recent *BABAR* measurements of the $\pi^0\gamma^*\gamma$ form factor at large momentum transfers [B. Aubert *et al.* (The *BABAR* Collaboration), Phys. Rev. D **80**, 052002 (2009)] are consistent with QCD, although they do suggest that the pion distribution amplitude may have more structure than usually assumed.

DOI: 10.1103/PhysRevD.83.054020 PACS numbers: 12.38.Bx, 12.39.St, 13.88.+e

I. INTRODUCTION

Despite a solid theory background [1–3], phenomenological success of QCD in exclusive reactions has been rather modest. A problem is that, since the quarks carry only some fractions of hadron momenta, virtualities of the internal lines of the hard subprocess appear to be essentially smaller than Q^2, the nominal momentum transfer to the hadron. As a result, at accessible Q^2, the bulk part of the hard QCD contribution comes from the regions where the ''hard'' virtualities are much smaller than the typical hadronic scale of 1 GeV^2 [4–6]. According to the factorization principle, contributions from such regions have to be subtracted from the hard coefficient function and included separately as additive ''soft'' or ''endpoint'' nonperturbative contributions. The standard power counting suggests that soft terms are suppressed by extra powers of $1/Q^2$. However, they do not involve small coefficients $\sim\alpha_s(Q)/\pi$ which are endemic for factorizable QCD contributions based on hard gluon exchanges. As the result, the onset of the perturbative regime may be postponed to very large momentum transfers.

The pion transition form factor $\gamma^*\gamma^{(*)} \to \pi^0$ with at least one virtual photon plays a very special rôle as it is the simplest hard exclusive process where the above- mentioned difficulties are absent or, at least, moderated. There is only one hadron (pion) involved, and the large Q^2 behavior of this form factor is determined [3] by the operator product expansion (OPE) of the product of two electromagnetic currents near the light cone which is very well studied in the context of inclusive deep-inelastic scattering. In this case the leading contribution to the hard coefficient function is of order one (i.e. not suppressed) as no gluon exchanges are involved, and at the same time soft (endpoint) contributions either do not exist—for the case of two virtual photons—or are likely to be suppressed, if one photon is real. These features make the pion transition form factor an ideal place to test the QCD factorization approach and determine the pion distribution amplitude (DA) which can then be used to describe other exclusive hard reactions. This task is as important as ever, the most high-profile application being at present to exclusive weak B-decays, $B \to \pi\ell\nu_\ell$, $B \to \pi\pi$, etc., which are the main source of precision information on quark flavor mixing parameters in the standard model. These are the aim of an extensive experimental study: It addresses the question whether there is new physics in flavor-changing processes and where it manifests itself.

Whereas the case of two virtual photons offers crucial simplifications for the theory, the transition form factors with one real and one virtual photon are much easier to study experimentally. They can be measured for spacelike momentum transfers in the process $e^+e^- \to e^+e^-\pi^0$, $\eta, \ldots$ and in $e^+e^- \to \gamma\pi^0$, $\eta, \ldots$ for timelike ones. Until 1995 only the CELLO data [7] were available at relatively low, spacelike momentum transfer: $Q^2 < 2.5$ GeV^2 for $\pi^0(\eta)\gamma^*\gamma$ and somewhat higher for $\eta'\gamma^*\gamma$. The covered region was extended to $Q^2 \sim 9$–15 GeV^2 by the CLEO Collaboration [8] which allowed, for the first time, a quantitative comparison with the perturbative QCD. The CLEO data appeared to be consistent with the predicted scaling behavior $\sim 1/Q^2$ setting in for momentum transfers of the order of a few GeV^2 and also suggested that the pion DA is somewhat broader compared to its asymptotic shape at large scales, which was, again, expected based on the corresponding studies using QCD sum rules. More recently, *BABAR* reported [9] a measurement of the timelike transition form factors $\eta\gamma^*\gamma$ and $\eta'\gamma^*\gamma$ at very large $q^2 = 112$ GeV^2. No significant tension with the theory was observed, although predictions in the timelike region are generally more difficult.

The situation changed in 2009 when the *BABAR* Collaboration presented [10] the measurement of the $\pi^0\gamma^*\gamma$ form factor up to photon virtualities of the order of 40 GeV^2. These new data created considerable

excitement in the theory community as they do not show the expected scaling behavior. The most popular explanation so far has been [11,12] that the pion DA has an unexpected "flat" shape and does not vanish at the end points. This explanation, on the one hand, triggered speculations on the breakdown of QCD factorization [13] and, on the other hand, claims that the *BABAR* data are in contradiction with light cone sum rules (LCSRs) and with the common wisdom on the lowest moments of the pion DA [14–16]. The aim of this work is to reexamine these claims by making an updated analysis of the $\pi^0\gamma^*\gamma$ form factor within the LCSR approach including up to six polynomials in the conformal expansion of the pion distribution amplitude and taking into account twist-six corrections. The photon emission at large distances is discussed in detail. The results are compared with the calculations of pion electromagnetic form factor and $B \to \pi\ell\nu$ decay in the same framework. Our conclusion is that the recent *BABAR* measurements [10] are consistent with QCD and with the bulk of the available information on the pion distribution amplitude. In particular we argue that the flat DA [11,12] is not warranted and in fact no conclusion on the endpoint behavior of the DA can be inferred on the basis of the existing experimental data.

The presentation is organized as follows. Sec. II contains a concise review of the QCD (collinear) factorization approach to the $\pi^0\gamma^*\gamma$ form factor and the existing information on the pion DA. The LCSR approach is motivated and explained in detail in Sec. III. In this work we go beyond the existing analysis [14,17–22] in two aspects. First, we calculate a new, twist-six contribution to LCSRs which proves to be sizeable. This contribution is related to photon emission from large distances for which we also derive the leading-order perturbative expression. Second, we extend the existing formalism to allow for the contributions of higher-order Gegenbauer polynomials, which allows one to consider DAs of arbitrary shape and also address the question of convergence of the Gegenbauer expansion which generated some confusion. The second task was already addressed in Ref. [14], but our expressions do not agree, unfortunately. Sec. IV contains the numerical study of the LCSRs to the next to leading order (NLO) accuracy. We consider various uncertainties of the method in some detail and provide error estimates for our predictions. The final Sec. V is reserved for a summary and conclusions.

II. QCD FACTORIZATION AND PION DA

The form factor $F_{\gamma^*\gamma^*\to\pi^0}(q_1^2, q_2^2)$ describing the pion transition in two (in general virtual) photons can be defined by the matrix element of the product of two electromagnetic currents,

$$\int d^4y e^{iq_1y}\langle\pi^0(p)|T\{j_\mu^{\rm em}(y)j_\nu^{\rm em}(0)\}|0\rangle = ie^2\varepsilon_{\mu\nu\alpha\beta}q_1^\alpha q_2^\beta F_{\gamma^*\gamma^*\to\pi^0}(q_1^2, q_2^2), \quad (1)$$

where

$$j_\mu^{\rm em}(y) = e_u\bar{u}(y)\gamma_\mu u(y) + e_d\bar{d}(y)\gamma_\mu d(y) + \ldots,$$

p is the pion momentum, and $q_2 = q_1 + p$. We will consider the spacelike form factor, in which case both photon virtualities are negative. The experimentally relevant situation is when one virtuality is large and the second one small (or zero). For definiteness we take

$$q_1^2 = -Q^2, \qquad q_2^2 = -q^2, \quad (2)$$

assuming that $q^2 \ll Q^2$. Most of the equations are written for $q^2 = 0$, and we use a shorthand notation $F_{\gamma^*\gamma\to\pi^0}(Q^2) \equiv F_{\gamma^*\gamma^*\to\pi^0}$ $(q_1^2 = -Q^2, q^2 = 0)$.

In general, a powerlike falloff of the form factor $F_{\gamma^*\gamma\to\pi^0}(Q^2)$ in the large-Q^2 limit can be generated by the three different possibilities of the large-momentum flow, as indicated schematically in Fig. 1 [23]. The first possibility, Fig. 1(a), corresponds to the hard subgraph that includes both photon vertices. This is the dominant contribution that starts at order $\sim 1/Q^2$. For the zero (or small, $q^2 \le \Lambda_{\rm QCD}^2$) virtuality of the second photon there exists another possibility, shown in Fig. 1(b): In this case the low-virtual photon is emitted at large distances and the large momentum flows through a subgraph corresponding to hard gluon exchange between the quarks. The power counting for this contribution shows that it is at most $\mathcal{O}(1/Q^4)$, i.e. subleading compared to the first regime. Finally, the third possible regime, shown in Fig. 1(c), corresponds to the Feynman mechanism, i.e. the possibility that the quark interacting with the hard photon carries almost all the momentum whereas the quark spectator is soft. This contribution can be thought of intuitively as an overlap of nonperturbative wave functions describing the initial (photon) and final (pion) states. In perturbation

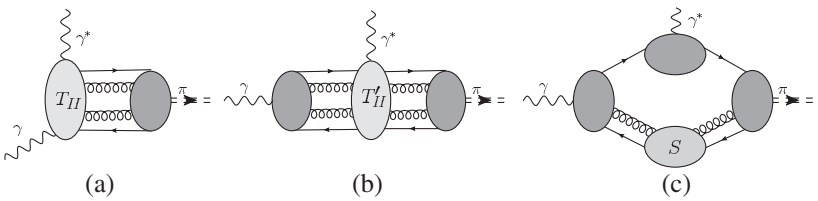

FIG. 1. Schematic structure of the QCD factorization for the $F_{\gamma^*\gamma\to\pi^0}(Q^2)$ factor.

theory, this contribution also scales as $\mathcal{O}(1/Q^4)$ in the large-Q^2 limit.

By construction, the contribution in Fig. 1(a) involves a time-ordered product of two electromagnetic currents at small light cone separations. Hence it can be studied using Wilson operator product expansion. The leading contribution $\mathcal{O}(1/Q^2)$ to the form factor corresponds to the contribution of the leading twist-two operators and can be written in the factorized form

$$F_{\gamma^*\gamma\to\pi^0}(Q^2) = \frac{\sqrt{2}f_\pi}{3} \times \int_0^1 dx T_H(x, Q^2, \mu, \alpha_s(\mu))\phi_\pi(x, \mu), \tag{3}$$

where $\phi_\pi(x, \mu)$, the pion distribution amplitude at the scale μ, is defined by the matrix element of the nonlocal quark-antiquark operator stretched along the lightlike direction n_μ, $n^2 = 0$:

$$\langle 0|\bar{q}(0)[0, \alpha n]\not{n}\gamma_5 q(\alpha n)|\pi^+(p)\rangle = if_\pi p\cdot n\int_0^1 dx e^{-ix\alpha p\cdot n}\phi_\pi(x, \mu). \tag{4}$$

Here and below $\bar{q}\not{n}\gamma_5 q = (1/\sqrt{2})[\bar{u}\not{n}\gamma_5 u - \bar{d}\not{n}\gamma_5 d]$. To this accuracy (leading twist), all gluon attachments to the hard subgraph [cf. Fig. 1(a)] can be absorbed in the path-ordered gauge link (Wilson line):

$$[0, \alpha n] = \mathrm{P}\exp\left\{-ig\int_0^\alpha dun^\mu A_\mu(un)\right\}. \tag{5}$$

The normalization is such that

$$\langle 0|\bar{q}(0)\gamma_\nu\gamma_5 q(0)|\pi^0(p)\rangle = if_\pi p_\nu, \quad \int_0^1 dx\phi_\pi(x, \mu) = 1, \tag{6}$$

where $f_\pi \simeq 131$ MeV is the usual pion decay constant.

The coefficient function in (3) is known in the modified minimal subtraction ($\overline{\mathrm{MS}}$) scheme to the NLO in the strong coupling [24–26]. Taking into account the symmetry of the pion DA $\phi_\pi(x) = \phi_\pi(1-x)$, it can be written as

$$T_H^{\mathrm{NLO}} = \frac{1}{xQ^2}\left\{1 + C_F\frac{\alpha_s(\mu)}{2\pi}\left[\frac{1}{2}\ln^2 x - \frac{x\ln x}{2(1-x)} - \frac{9}{2} + \left(\frac{3}{2} + \ln x\right)\ln\frac{Q^2}{\mu^2}\right]\right\}. \tag{7}$$

Symmetry properties of the renormalization-group (RG) equation which governs the scale dependence of the pion DA [2,3] suggest the series expansion of the DA in Gegenbauer polynomials

$$\phi_\pi(x, \mu) = \sum_{n=0}^\infty a_n(\mu)\varphi_n(x), \quad \varphi_n(x) = 6x(1-x)C_n^{3/2}(2x-1). \tag{8}$$

The first coefficient $a_0(\mu) = 1$ is fixed by the normalization condition whereas the remaining ones, $a_n(\mu_0)$ for $n = 2, 4, \ldots$, have to be determined by some nonperturbative method (or taken from experiment).

To leading order (LO), the Gegenbauer coefficients are renormalized multiplicatively whereas, to the NLO accuracy, the mixing pattern becomes more complicated. One obtains [27–32]

$$a_n^{\mathrm{NLO}}(\mu) = a_n(\mu_0)E_n^{\mathrm{NLO}}(\mu, \mu_0) + \frac{\alpha_s(\mu)}{4\pi} \times \sum_{k=0}^{n-2} a_k(\mu_0)E_k^{\mathrm{LO}}(\mu, \mu_0)d_n^k(\mu, \mu_0). \tag{9}$$

Explicit expressions for the RG factors $E_n^{(\mathrm{N})\mathrm{LO}}(\mu, \mu_0)$ and the off-diagonal mixing coefficients $d_n^k(\mu, \mu_0)$ in the $\overline{\mathrm{MS}}$ scheme are collected in Appendix A.

The next-to-next-to-leading-order (NNLO) calculations of the transition pion form factor exist in the so-called conformal scheme $\overline{\mathrm{CS}}$ [33,34], but they cannot be converted to $\overline{\mathrm{MS}}$ lacking the full NNLO result for the trace anomaly term, which is so far not available. An extensive discussion of scheme dependence can be found in Refs. [31–33].

The existing information on the pion DA comes from QCD sum rules, lattice calculations, and light cone sum rules. The first nontrivial Gegenbauer coefficient a_2 is related to the second moment of the DA,

$$\langle\xi^2\rangle \equiv \int_0^1 dx(2x-1)^2\phi_\pi(x), \qquad a_2 = \frac{7}{12}(5\langle\xi^2\rangle - 1), \tag{10}$$

and can be evaluated as a matrix element of the local operator with two derivatives between vacuum and the pion state. There exists overwhelming evidence that this coefficient is positive, meaning that the pion DA is broader than its asymptotic expression $\phi_\pi^{\mathrm{as}} = 6x(1-x)$; see Table I.

Such calculations were pioneered in 1981 by Chernyak and Zhitnitsky [35], who derived the corresponding sum rule and obtained $a_2 \sim 0.5$ at the scale of order $\mu^2 = 1 - 1.5$ GeV^2. Extrapolating this number to a very low scale $\mu^2 = 0.25$ GeV^2 and adding a simplifying assumption that higher-order coefficients $a_4, \ldots$ vanish, they have formulated a simple model for the low-energy pion DA, which has become known as the Chernyak-Zhitnitsky (CZ) model:

TABLE I. The Gegenbauer moment $a_2(\mu^2)$. The CZ model involves $a_2 = 2/3$ at the low scale $\mu = 500$ MeV; for the discussion of the extrapolation to higher scales, see Ref. [20]. The abbreviations stand for: QCDSR: QCD sum rules; NLC: nonlocal condensates; LCSR: light cone sum rules; R: renormalon model for twist-four corrections; LQCD: lattice calculation; $N_f = 2(+1)$: calculation using $N_f = 2(+1)$ dynamical quarks; CW: nonperturbatively $\mathcal{O}(a)$-improved CloverWilson fermion action; DWF: domain wall fermions. For convenience we present the results for two scales, $\mu = 1$ GeV and $\mu = 2$ GeV; the relation is calculated in NLO.

Method	$\mu = 1$ GeV	$\mu = 2$ GeV	References
LO QCDSR, CZ model	0.56	0.39	[35,36]
QCDSR	$0.26^{+0.21}_{-0.09}$	$0.18^{+0.15}_{-0.06}$	[37]
QCDSR	0.28 ± 0.08	0.19 ± 0.06	[38]
QCDSR, NLC	0.19 ± 0.06	0.13 ± 0.04	[19,39,40]
$F_{\pi\gamma\gamma^*}$, LCSR	0.19 ± 0.05	0.12 ± 0.03 ($\mu = 2.4$)	[18]
$F_{\pi\gamma\gamma^*}$, LCSR	0.32	0.21 ($\mu = 2.4$)	[20]
$F_{\pi\gamma\gamma^*}$, LCSR, R	0.44	0.31	[41]
$F_{\pi\gamma\gamma^*}$, LCSR, R	0.27	0.19	[22]
$F_\pi^{\rm em}$,LCSR	$0.24 \pm 0.14 \pm 0.08$	$0.17 \pm 0.10 \pm 0.05$	[42,43]
$F_\pi^{\rm em}$, LCSR, R	0.20 ± 0.03	0.14 ± 0.02	[44]
$F_{B\to\pi\ell\nu}$, LCSR	0.19 ± 0.19	0.13 ± 0.13	[45]
$F_{B\to\pi\ell\nu}$, LCSR	0.16	0.11	[46]
LQCD, $N_f = 2$, CW	0.289 ± 0.166	0.201 ± 0.114	QCDSF/UKQCD [47]
LQCD, $N_f = 2 + 1$, DWF	0.334 ± 0.129	0.233 ± 0.088	RBS/UKQCD [48]

$$\phi_\pi^{\rm CZ}(x) = 30x(1-x)(2x-1)^2 = 6x(1-x)\left[1 + \frac{2}{3}C_2^{3/2}(2x-1)\right]. \quad (11)$$

This model corresponds to a very asymmetric momentum fraction distribution which vanishes at the point where the pion momentum is shared equally between the quark and the antiquark $\phi_\pi^{\rm CZ}(x = 1/2) = 0$. The striking difference of the CZ model and the asymptotic DA has been fuelling an extensive and sometimes heated discussion for many years.

Newer estimates of a_2 following the CZ approach yield a somewhat smaller value [37,38], $a_2(1\ {\rm GeV}) \sim 0.3$, the difference being due to a combination of several factors: writing the sum rules for a_2 directly instead of the second moment $\langle\xi^2\rangle$, taking into account the NLO corrections, and using slightly different values of the parameters.

Light cone sum rules [49–51] are a modification of the general Shifman-Vainshtein-Zakharov approach [52], in which the pion DA serves as the main input in calculations of form factors (or hadron matrix elements). The Gegenbauer coefficient a_2 is not calculated directly but is extracted from the comparison of the LCSR calculations with the experimental data. Note that, in the case of the pion transition form factor, these fits are based on CLEO data [8] only. The results for a_2 are consistent with the direct calculations; see Table I.

Finally, two independent lattice calculations of a_2 are now available [47,48]. The largest part of the uncertainty in these results is due to the chiral extrapolation. Overall, the results in Table I show a consistent picture,

$$a_2^{\rm NLO}(\mu^2 = 1\ {\rm GeV}^2) = 0.25 \pm 0.10, \quad (12)$$

and one can expect that the accuracy will increase in the near future when lattice calculations with physical pion mass become available.

Very little, unfortunately, is known about the next Gegenbauer coefficient, a_4. The LCSR fits of heavy meson decay form factors indicate a small positive value, $a_4 \sim 0.04$ [46], whereas the similar approach applied to the pion transition form factor (CLEO data only) favors small negative values [20,22,41]. Lattice calculations of this coefficient suffer from large (lattice) artifacts in the operator renormalization and are not feasible at present.

The calculation of a_4 within the QCD sum rule approach has been attempted in the so-called nonlocal condensate (NLC) model [19,39,40], which involves a resummation of a tower of condensates of a certain type. This approach leads to a sizeable negative value $a_4 \sim -0.1$, which is included in the so-called Bakulev-Mikhailov-Stefanis model of the pion DA. A large negative value for a_4 in the NLC approach can be traced back to the basic feature of this model, that nonperturbative corrections to the DA get smeared over a *finite* interval of momentum fractions $\Delta x \sim \lambda_q^2/(2M^2) \sim 0.2$, where $\lambda_q^2 = \langle\bar{q}D^2q\rangle/\langle\bar{q}q\rangle \sim 0.4\ {\rm GeV}^2$ is the average virtuality of quarks in QCD vacuum and $M^2 \sim 1\ {\rm GeV}^2$ is the Borel parameter. In our opinion, appearance of Δx is an artifact of the NLC model: Contributions of this type would produce "bumps" at large values of the Bjorken variable in quark parton distributions in the nucleon [53] (which are absent), and also a finite smearing proves not sufficient to cure the QCD

sum rules for heavy-to-light decay form factors [54] (which is the reason why this technique was eventually abandoned and replaced by LCSRs). It seems much more natural to assume that the nonperturbative contributions get smeared over the whole interval of momentum fractions $0 < x < 1$. A possible mechanism for such "complete" smearing is considered in the example of a photon DA in Appendix B in Ref. [55]. We believe, therefore, that the NLC-model-based predictions for a_4 have to be viewed with caution.

Last but not least, we mention the LCSR calculation [50] for the pion DA in the middle point:

$$\phi_\pi(x = 0.5, \mu^2 = 1\ \text{GeV}^2) = 1.2 \pm 0.3, \qquad (13)$$

which is the only available result beyond the Gegenbauer expansion. This result excludes a large "dip" in the pion DA in the center region and thus contradicts the CZ and Bakulev-Mikhailov-Stefanis models. It is consistent, however, with most of the parametrizations of the pion DA that are used in vast literature on B-decays. Smaller values of $\phi_\pi(x = 0.5)$ are also strongly disfavored by numerous LCSR calculations of pion-hadron couplings $g_{\pi NN}$, $g_{\pi DD^*}$, $g_{\rho\omega\pi}$, ...; see e.g. [50,56–60].

It has been suggested [11,12] that the *BABAR* data [10] indicate an unusual flat DA $\phi_\pi(x) \simeq 1$ which does not vanish at the end points so that the Gegenbauer expansion is not convergent (more precisely: not uniformly convergent at the end points). We believe that this conclusion is not warranted and in fact no conclusion on the endpoint behavior of the pion DA can be inferred on the basis of the existing experimental data.

To explain our statement, let us examine the argumentation in [11] more closely. It is based on the elegant model for the transition form factor suggested by Musatov and Radyushkin (MR) in an earlier work [23], which is derived from the exact two-body (e.g. quark-antiquark) contribution in the noncovariant light cone formalism of Brodsky and Lepage [3] under certain simplifying assumptions on the shape of the pion wave function:

$$F^{\text{MR}}_{\gamma^*\gamma\to\pi^0}(Q^2) = \frac{\sqrt{2}f_\pi}{3Q^2}\int_0^1 \frac{dx}{x}\phi_\pi(x)\left[1 - \exp\left(-\frac{xQ^2}{2\bar{x}\sigma}\right)\right]. \qquad (14)$$

The first term in the square brackets corresponds to the usual leading-order contribution to Fig. 1(a), whereas the second term is entirely a soft contribution of the type in Fig. 1(c). Note that this second term is exponentially small in Q^2 for each finite quark momentum fraction, so it is absent in any order of the operator product expansion. Using Eq. (14) with $\sigma = 0.53\ \text{GeV}^2$ [11] and the flat pion DA $\phi_\pi(x) = 1$ allows one to describe the apparent scaling violation in the *BABAR* data, as illustrated by the solid curve in Fig. 2.

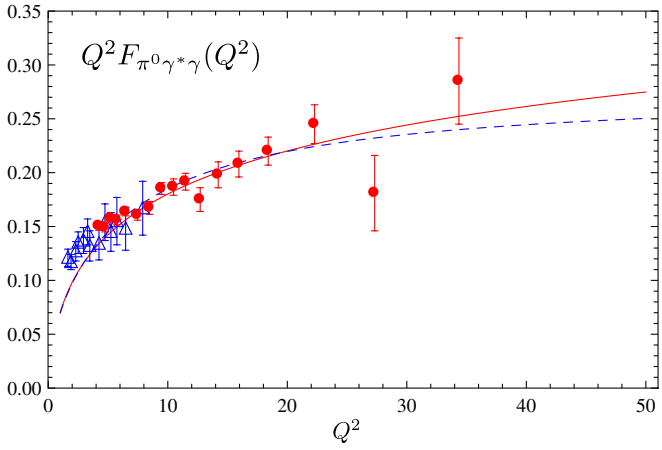

FIG. 2 (color online). Pion transition form factor in the MR model (14) calculated using flat pion DA (solid [red] curve) and CZ-type DA with $a_2 = 0.5$ and higher Gegenbauer moments set to zero (dashed [blue] curve). The nonperturbative parameter $\sigma = 0.53\ \text{GeV}^2$ in both cases. The experimental data are from [10] (full circles) and [8] (open triangles).

The caveat with this argument (and a very similar argumentation in Ref. [12]) is that flat DA is not necessary; in fact a CZ-type DA with $a_2 = 0.5$,

$$\phi_\pi(x) = 6x(1-x)\left[1 + \frac{1}{2}C_2^{3/2}(2x-1)\right],$$

yields a very similar (or even better) description of the data; see the dashed (blue) curve in Fig. 2. Moreover, it is seen that the two DA models can hardly be discriminated at all unless precise data with $Q^2 > 20\ \text{GeV}^2$ are available.

It is easy to see why this happens. The flat DA $\phi_\pi^{\text{flat}}(x) = 1$ can be expanded in Gegenbauer polynomials as follows:

$$1 = \sum_{k=0,2,\ldots} a_k^{\text{flat}}\varphi_k(x), \quad a_k^{\text{flat}} = \frac{2(2k+3)}{3(k+1)(k+2)}. \qquad (15)$$

This equation has to be understood in the sense of distributions: The equality holds when both sides are integrated with a test function that is finite (or does not increase too fast) at the end points.

In perturbation theory (LO), the form factor is proportional to the sum of the Gegenbauer coefficients,

$$\int_0^1 \frac{dx}{x}\phi_\pi(x) = 3[1 + a_2 + a_4 + \ldots].$$

For the flat DA, this series diverges, which motivates introduction of a certain regulator, e.g. the soft correction given by the second, exponential, term in Eq. (14) or effective quark mass in Ref. [12]. Our observation is, however, that *if* such a regulator is included, the Gegenbauer expansion for the form factor is converging very rapidly and contributions of higher-order terms in this series are in fact negligible. For illustration, consider the MR model with a flat DA for, say, $Q^2 = 20\ \text{GeV}^2$, and

check how much is being contributed by each successive Gegenbauer polynomial. One obtains

$$Q^2 F^{\mathrm{MR,flat}}_{\gamma^*\gamma\to\pi^0}(Q^2=20) = \frac{\sqrt{2}f_\pi}{3}\cdot 3.565\,13$$
$$= \frac{\sqrt{2}f_\pi}{3}[2.724 + 0.649 + 0.162 + 0.028 + \ldots], \qquad (16)$$

where the first term on the right-hand side is the contribution of the asymptotic DA, the second term is due to a_2^{flat}, etc. One sees that all contributions beyond $n = 4$ are tiny.

Our conclusion is that a good description of the *BABAR* data [10] achieved in [11,12] is that it is not due to an unusual endpoint behavior of the DA, but rather to a (model-dependent) large nonperturbative soft correction to the form factor. Such a large correction effectively suppresses contributions of higher order terms in the Gegenbauer expansion and makes the question of the endpoint behavior of the pion DA irrelevant. The problem is, therefore, whether such a large nonperturbative correction can be expected, and whether it can be estimated in a model-independent way. This is the question that we address in the next section.

III. LIGHT CONE SUM RULES FOR THE PION-PHOTON TRANSITION

A. Dispersion approach

The technique that we adopt in what follows was originally suggested by Khodjamirian in [17]. It is to calculate the pion transition form factor for two large virtualities, Q^2 and q^2, using the OPE, and make the analytic continuation to the real photon limit $q^2 = 0$ using dispersion relations. In this way, explicit evaluation of contributions of the type in Figs. 1(b) and 1(c) is avoided (since they do not contribute for sufficiently large q^2) and effectively replaced by certain assumptions on the physical spectral density in the q^2-channel.

The starting observation [17] is that $F_{\gamma^*\gamma^*\to\pi^0}(Q^2, q^2)$ satisfies an unsubtracted dispersion relation in the variable q^2 for fixed Q^2. Separating the contribution of the lowest-lying vector mesons ρ, ω, one can write

$$F_{\gamma^*\gamma^*\to\pi^0}(Q^2,q^2) = \frac{\sqrt{2}f_\rho F_{\gamma^*\rho\to\pi^0}(Q^2)}{m_\rho^2+q^2} + \frac{1}{\pi}\int_{s_0}^{\infty} ds \frac{\mathrm{Im}F_{\gamma^*\gamma^*\to\pi^0}(Q^2,-s)}{s+q^2}, \qquad (17)$$

where s_0 is a certain effective threshold. Here, the ρ and ω contributions are combined in one resonance term assuming $m_\rho \simeq m_\omega$ and the zero-width approximation is adopted; $f_\rho \sim 200$ MeV is the usual vector meson decay constant. Note that, since there are no massless states, the real photon limit is recovered by the simple substitution $q^2 \to 0$ in (17).

On the other hand, the same form factor can be calculated using QCD perturbation theory and the OPE. The QCD result satisfies a similar dispersion relation:

$$F^{\mathrm{QCD}}_{\gamma^*\gamma^*\to\pi^0}(Q^2,q^2) = \frac{1}{\pi}\int_0^\infty ds \frac{\mathrm{Im}F^{\mathrm{QCD}}_{\gamma^*\gamma^*\to\pi^0}(Q^2,-s)}{s+q^2}. \qquad (18)$$

The basic assumption of the method is that the physical spectral density above the threshold s_0 coincides with the QCD spectral density as given by the OPE:

$$\mathrm{Im}\,F_{\gamma^*\gamma^*\to\pi^0}(Q^2,-s) = \mathrm{Im}F^{\mathrm{QCD}}_{\gamma^*\gamma^*\to\pi^0}(Q^2,-s) \qquad (19)$$

for $s > s_0$. This is the usual approximation of local quark-hadron duality.

We expect that the QCD result reproduces the "true" form factor for large values of q^2. Equating the two representations (17) and (18) at $q^2 \to -\infty$ and subtracting the contributions of $s > s_0$ from both sides, one obtains

$$\sqrt{2}f_\rho F_{\gamma^*\rho\to\pi^0}(Q^2) = \frac{1}{\pi}\int_0^{s_0} ds \mathrm{Im}F^{\mathrm{QCD}}_{\gamma^*\gamma^*\to\pi^0}(Q^2,-s). \qquad (20)$$

This relation explains why s_0 is usually referred to as the interval of duality (in the vector channel). The (perturbative) QCD spectral density $\mathrm{Im}F^{\mathrm{QCD}}_{\gamma^*\gamma^*\to\pi^0}(Q^2,-s)$ is a smooth function and does not vanish at small $s \to 0$. It is very different from the physical spectral density $\mathrm{Im}F_{\gamma^*\gamma^*\to\pi^0}(Q^2,-s) \sim \delta(s-m_\rho^2)$. However, the integral of the QCD spectral density over a certain region of energies coincides with the integral of the physical spectral density over the same region; in this sense, the QCD description of correlation functions in terms of quark and gluons is dual to the description in terms of hadronic states.

In practical applications of this method, one uses an additional trick, borrowed from QCD sum rules [52], which allows one to reduce the sensitivity on the duality assumption in Eq. (19) and also suppress contributions of higher orders in the OPE. The idea is essentially to make the matching between the true and calculated form factor at a finite value $q^2 \sim 1$–2 GeV^2 instead of the $q^2 \to \infty$ limit. This is done by going over to the Borel representation $1/(s+q^2) \to \exp[-s/M^2]$, the net effect being the appearance of an additional weight factor under the integral:

$$\sqrt{2}f_\rho F_{\gamma^*\rho\to\pi^0}(Q^2) = \frac{1}{\pi}\int_0^{s_0} ds e^{-(s-m_\rho^2)/M^2} \times \mathrm{Im}F^{\mathrm{QCD}}_{\gamma^*\gamma^*\to\pi^0}(Q^2,-s). \qquad (21)$$

Varying the Borel parameter within a certain window, usually 1–2 GeV^2, one can test the sensitivity of the results to the particular model of the spectral density.

With this refinement, substituting Eq. (21) in (17) and using Eq. (19), one obtains for $q^2 \to 0$ [17]

$$F^{\rm LCSR}_{\gamma^*\gamma\to\pi^0}(Q^2) = \frac{1}{\pi}\int_0^{s_0}\frac{ds}{m_\rho^2}\,{\rm Im}F^{\rm QCD}_{\gamma^*\gamma^*\to\pi^0}(Q^2,-s)e^{(m_\rho^2-s)/M^2} + \frac{1}{\pi}\int_{s_0}^{\infty}\frac{ds}{s}\,{\rm Im}F^{\rm QCD}_{\gamma^*\gamma^*\to\pi^0}(Q^2,-s). \quad (22)$$

This expression contains two nonperturbative parameters—vector meson mass m_ρ^2 and effective threshold $s_0 \simeq 1.5$ GeV^2—as compared to the pure QCD calculation, and the premium is that one does not need to evaluate the contributions of Figs. 1(b) and 1(c) explicitly: They are taken into account effectively via the nonperturbative modification of the spectral density.

As an illustration, consider the leading twist QCD expression at the leading order:

$$F^{\rm QCD}_{\gamma^*\gamma^*\to\pi^0}(Q^2,q^2) = \frac{\sqrt{2}f_\pi}{3}\int_0^1\frac{dx\phi_\pi(x)}{xQ^2+\bar{x}q^2}. \quad (23)$$

In this case, the momentum fraction integral can easily be converted to the form of a dispersion relation by the change of variables $x \to s = Q^2\bar{x}/x$. The resulting LO and leading twist LCSR expression is [17]

$$F^{\rm LCSR}_{\gamma^*\gamma\to\pi^0}(Q^2) = \frac{\sqrt{2}f_\pi}{3}\left\{\int_0^{x_0}\frac{dx\phi_\pi(x)}{\bar{x}m_\rho^2}e^{(\bar{x}m_\rho^2-xQ^2)/(\bar{x}M^2)} + \frac{1}{Q^2}\int_{x_0}^1\frac{dx\phi_\pi(x)}{x}\right\}, \quad (24)$$

where

$$x_0 = \frac{s_0}{s_0+Q^2}. \quad (25)$$

Note that the modification of the perturbative expression concerns only the region $x < x_0 \sim s_0/Q^2$, so this is a soft contribution in our classification. Since $\phi_\pi(x) \sim x$ for $x \to 0$, this contribution [first term in (24)] corresponds to a power correction of the order of s_0/Q^4 for $Q^2 \to \infty$, in agreement with usual reasoning based on the power counting.

B. NLO perturbative corrections

The NLO perturbative corrections to the $\gamma^*\gamma^*\pi^0$ form factor for arbitrary photon virtualities were calculated in Refs. [24–26]:

$$F^{\rm QCD}_{\gamma^*\gamma^*\to\pi^0}(Q^2,q^2) = \frac{\sqrt{2}f_\pi}{3}\int_0^1\frac{dx\phi_\pi(x)}{xQ^2+\bar{x}q^2}\times\left[1+\frac{C_F\alpha_s}{2\pi}t(\bar{x},w)\right]. \quad (26)$$

The function $t(x,w)$ where $w = Q^2/(Q^2+q^2)$ is given in Eq. (5.2) in Ref. [25].

Following Ref. [18] we write the required imaginary part of $F^{\rm QCD}_{\gamma^*\gamma^*\to\pi^0}(Q^2,q^2)$ as the sum of terms corresponding to the expansion of the pion DA $\phi_\pi(x,\mu)$ in Gegenbauer polynomials (8):

$$\frac{1}{\pi}{\rm Im}F^{\rm QCD}_{\gamma^*\gamma^*\to\pi^0}(Q^2,-s) = \frac{\sqrt{2}f_\pi}{3}\sum_{n=0}^{\infty}a_n(\mu)\left[\rho_n^{(0)}(Q^2,s) + \frac{C_F\alpha_s}{2\pi}\rho_n^{(1)}(Q^2,s;\mu)\right], \quad (27)$$

where the LO partial spectral density is proportional to the pion DA:

$$\rho_n^{(0)}(Q^2,s) = \frac{\varphi_n(x)}{Q^2+s}, \qquad x = \frac{Q^2}{Q^2+s}. \quad (28)$$

The NLO spectral density

$$\rho_n^{(1)}(Q^2,s) = \int_0^1 dx\varphi_n(x)\frac{1}{\pi}\,{\rm Im}\left[\frac{t(\bar{x},w)}{xQ^2+\bar{x}q^2}\right]_{q^2=-s} \quad (29)$$

can be written in the following form:

$$\rho_n^{(1)}(Q^2,s) = \frac{1}{2(Q^2+s)}\left\{\left[-3[1+2(\psi(2)-\psi(2+n))] + \frac{\pi^2}{3} - \ln^2\left(\frac{\bar{x}}{x}\right) - \tilde{\gamma}_n^{(0)}\ln\left(\frac{s}{\mu^2}\right)\right]\varphi_n(x) + \tilde{\gamma}_n^{(0)}\int_0^{\bar{x}}du\frac{\varphi_n(u)-\varphi_n(\bar{x})}{u-\bar{x}} - 2\left[\int_x^1 du\frac{\varphi_n(u)-\varphi_n(x)}{u-x}\ln\left(1-\frac{x}{u}\right) + (x\to\bar{x})\right]\right\}, \quad (30)$$

where, as above, $x \equiv Q^2/(Q^2+s)$, $\psi(x) = d\ln\Gamma(x)/dx$ and $\tilde{\gamma}_n^{(0)}$ is related to the leading-order anomalous dimension $\gamma_n^{(0)}$ (A4) as

$$\gamma_n^{(0)} \equiv 2C_F\tilde{\gamma}_n^{(0)}. \quad (31)$$

Our result is similar but does not agree with the corresponding expression in Ref. [14]. The difference is that the first term in the second line in (30) is not symmetrized in $(x\to\bar{x})$ and hence the whole expression in braces is not symmetric under this substitution. We have checked that the spectral densities in (30) reproduce the corresponding expressions for $n = 0, 2, 4$ in [18]: $\rho_n^{(1)}(Q^2,s) = -A_n$. We also checked by numerical integration for $n \le 12$ that the dispersion relation

$$\int_0^1 dx\frac{\varphi_n(x)t(\bar{x},w)}{xQ^2+\bar{x}q^2} = \int_0^\infty\frac{ds}{s+q^2}\rho_n^{(1)}(Q^2,s) \quad (32)$$

is indeed satisfied.

As noticed in [14], the integrals appearing in Eq. (30) can be expanded in terms of $\varphi_n(x)$ with rational coefficients:

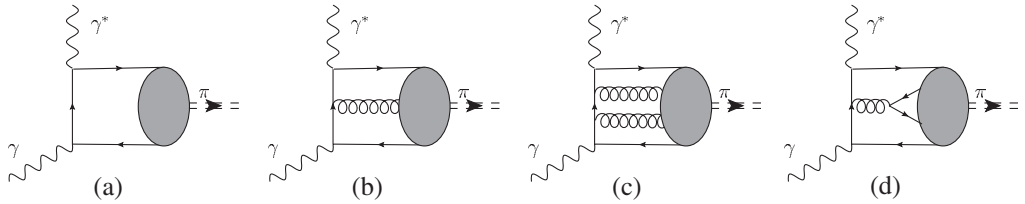

FIG. 3. Twist-four corrections to the pion transition form factor.

$$\left[\int_x^1 du\,\frac{\varphi_n(u)-\varphi_n(x)}{u-x}\ln(1-\frac{x}{u})+(x\to\bar{x})\right] = -\sum_{k=0,2,\ldots}^{n} G_n^k\varphi_k(x), \tag{33}$$

$$\int_0^{\bar{x}} du\,\frac{\varphi_n(u)-\varphi_n(\bar{x})}{u-\bar{x}} = -3\bar{x}+\sum_{k=0,1,\ldots}^{n} H_n^k\varphi_k(x). \tag{34}$$

The matrices G_n^k and H_n^k can easily be calculated using orthogonality relations for the Gegenbauer polynomials, e.g.

$$H_n^k = \mathcal{N}_k^{-1}\int_0^1 dx C_k^{3/2}(2x-1) \times\left[\int_0^{\bar{x}} du\,\frac{\varphi_n(u)-\varphi_n(\bar{x})}{u-\bar{x}}+3\bar{x}\right], \tag{35}$$

where $\mathcal{N}_k = (3/2)(k+1)(k+2)/(2k+3)$. Explicit expressions for $n, k \le 12$ are collected in Appendix B.

C. Twist-four corrections

Twist-four corrections to the form factor, by definition, correspond to the contributions of twist-four operators in the OPE of the time-ordered product of the two electromagnetic currents in Eq. (1). Such contributions are of order $1/Q^4$, but, as we will see later, they are not the only ones that have to be taken into account to this accuracy: Twist counting does not coincide in the present case with the counting of powers of large momentum, so they should not be mixed.

Intuitively, twist-four effects can be thought of as due to quark transverse momentum (or virtuality) in the handbag diagram shown in Fig. 3(a) and quark-antiquark-gluon components in the pion wave function, Fig. 3(b). These two contributions are related by exact QCD equations of motion [61]; hence they must be taken into account simultaneously. The corresponding calculation was done in Ref. [17]. The result (for two virtual photons) can be written as

$$F_{\gamma^*\gamma^*\to\pi^0}(Q^2,q^2) = \frac{\sqrt{2}f_\pi}{3}\left(\int_0^1 dx\,\frac{\phi_\pi(x)}{Q^2x+q^2\bar{x}} - \int_0^1 dx\,\frac{\mathbb{F}_\pi(x)}{(Q^2x+q^2\bar{x})^2}\right), \tag{36}$$

and therefore

$$\frac{1}{\pi}\,\mathrm{Im}F_{\gamma^*\gamma^*\to\pi^0}(Q^2,-s) = \frac{\sqrt{2}f_\pi}{3}\left[\frac{\phi_\pi(x)}{s+Q^2}-\frac{1}{Q^2}\frac{d\mathbb{F}_\pi(x)}{ds}\right], \tag{37}$$

with the usual substitution $x \equiv Q^2/(s+Q^2)$. The first term on the right-hand side. of (36) and (37) is the leading order twist-two contribution, and $\mathbb{F}_\pi(x)$ is given in terms of the twist-four pion DAs

$$\mathbb{F}_\pi(x,\mu) = \frac{1}{4}\phi_{4;\pi}(x) + \int_0^{\bar{x}} d\alpha_1\int_0^x d\alpha_2\left[\frac{1}{\alpha_3}\times\left(\frac{x-\bar{x}+\alpha_1-\alpha_2}{\alpha_3}\Phi_{4;\pi}(\underline{\alpha}) - \tilde{\Phi}_{4;\pi}(\underline{\alpha})\right)\right]_{\alpha_3=1-\alpha_1-\alpha_2}, \tag{38}$$

where $\underline{\alpha} = \{\alpha_1,\alpha_2,\alpha_3\}$. The two-particle twist-four DA $\phi_{4;\pi}(x)$ is defined by the light cone expansion $y^2\to 0$ of the bilocal quark-antiquark operator [38,61,62]

$$\langle 0|\bar{q}(0)\gamma_\mu\gamma_5 q(y)|\pi(p)\rangle = if_\pi p_\mu\int_0^1 dx e^{-ixp\cdot y}\times\left[\phi_\pi(x)+\frac{y^2}{16}\phi_{4;\pi}(x)\right]+\ldots, \tag{39}$$

and the three-particle DAs $\Phi_{4;\pi}(\underline{\alpha})$, $\tilde{\Phi}_{4;\pi}(\underline{\alpha})$ correspond to the matrix elements

$$\begin{aligned}&\langle 0|\bar{q}(0)\gamma_\mu\gamma_5 gG_{\alpha\beta}(vn)q(un)|\pi(p)\rangle \\ &\quad = p_\mu(p_\alpha n_\beta - p_\beta n_\alpha)\frac{1}{pn}f_\pi\Phi_{4;\pi}(u,v;pn)+\ldots, \\ &\langle 0|\bar{q}(0)\gamma_\mu ig\tilde{G}_{\alpha\beta}(vn)q(un)|\pi(p)\rangle \\ &\quad = p_\mu(p_\alpha n_\beta - p_\beta n_\alpha)\frac{1}{pn}f_\pi\tilde{\Phi}_{4;\pi}(u,v;pn)+\ldots,\end{aligned} \tag{40}$$

with the shorthand notation

$$\mathcal{F}(u,v;pn) = \int \mathcal{D}\underline{\alpha}\, e^{-ipn(u\alpha_1+v\alpha_3)}\mathcal{F}(\underline{\alpha}).$$

The Wilson lines in the definitions of the nonlocal operators in (39) and (40) are not shown for brevity. The integration measure is defined as $\mathcal{D}\underline{\alpha} = d\alpha_1 d\alpha_2 d\alpha_3\times\delta(1-\alpha_1-\alpha_2-\alpha_3)$, and the dots denote contributions

of other Lorentz structures that drop out and also terms of twist-five and higher. Our notation follows Ref. [38].

Strictly speaking, there also exist twist-four contributions from the wave function components containing two gluons or an extra quark-antiquark pair, see Figs. 3(c) and 3(d), but they are usually assumed to be small and neglected. The relevant argument is based on the specific property of four-particle twist-four distributions: They do not allow for a factorization in terms of two-particle distributions and, say, quark or gluon condensate.

Higher-twist DAs can be studied using the conformal partial wave expansion, which is a generalization of the Gegenbauer polynomial expansion for the leading twist DAs [61]. The contribution of the lowest conformal spin (asymptotic DAs) is

$$\mathbb{F}_\pi^{\rm as}(x,\mu) = \left(\frac{50}{3}+10\right)\delta_\pi^2(\mu)x^2(1-x)^2 = \frac{80}{3}\delta_\pi^2(\mu)x^2(1-x)^2, \tag{41}$$

where the first and the second contribution in parentheses are the contributions of the two-particle and three-particle DAs in (38), respectively. We stress that these two contributions are related by exact equations of motion, taking into account e.g. the twist-four correction to the handbag diagram and omitting contributions of three-particle DAs is inconsistent with QCD. One can show [34] that the next-to-leading-order conformal spin contributions to the relevant DAs do not contribute to $\mathbb{F}_\pi(x,\mu)$, sothis result is valid to NLO in the conformal expansion. The coupling δ_π^2 is defined by the matrix element

$$\langle 0|\bar q g\tilde G_{\mu\nu}\gamma^\nu q|\pi(p)\rangle = ip_\mu f_\pi\delta_\pi^2, \qquad \delta_\pi^2(\mu) = \left(\frac{\alpha_s(\mu)}{\alpha_s(\mu_0)}\right)^{32/(9\beta_0)}\delta_\pi^2(\mu_0). \tag{42}$$

This parameter was estimated using the QCD sum rule approach in [63] (see also [20]):

$$\delta_\pi^2(\mu^2=1\ {\rm GeV}^2)\simeq 0.2\ {\rm GeV}^2. \tag{43}$$

D. Twist-six corrections

The calculation of twist-six corrections to the transition form factor presents a new result of this work. To explain why such corrections may be important, consider an example of the Feynman diagram shown in Fig. 4(a). The broken quark line with crosses stands for the quark condensate. If both photon virtualities are large, this diagram contributes to the OPE of the product of the two electromagnetic currents (the so-called cat's-ears contribution) which involves the twist-six four-quark pion DA in the factorization approximation: One quark-antiquark pair is put in the condensate and the other one forms a twist-three chiral-odd quark-antiquark DA. Explicit calculation gives (cf. [17])

$$F^{\rm Fig.4a}_{\gamma^*\gamma^*\to\pi^0}(Q^2,q^2) = \frac{\sqrt{2}f_\pi}{3}\frac{32\pi\alpha_s\langle\bar qq\rangle^2}{9f_\pi^2q^2Q^2}\int_0^1\frac{dx\phi^p_{3;\pi}(x)}{xQ^2+\bar xq^2}, \tag{44}$$

where [38,61,62]

$$\langle 0|\bar q(0)i\gamma_5 q(\alpha n)|\pi(p)\rangle = \frac{f_\pi m_\pi^2}{m_u+m_d}\times\int_0^1 dx e^{-ix\alpha pn}\phi^p_{3;\pi}(x). \tag{45}$$

The DA $\phi^p_{3;\pi}(x)$ is related to the contribution of three-particle (quark-antiquark-gluon) Fock state by equations of motion [61]. If the contributions of the twist-three three-particle DA are neglected, $\phi^p_{3;\pi}(x)=1$ must be taken [38,61,62]. In Eq. (44) we used the Gell-Mann-Oakes-Renner relation $(m_u+m_d)(\langle\bar uu\rangle+\langle\bar dd\rangle) = -f_\pi^2m_\pi^2$, which is exact in the chiral limit.

For the case of two equal large virtualities $q^2=Q^2$, this contribution is of order $\langle\bar qq\rangle^2/Q^6$, so it is suppressed by two extra powers of $1/Q^2$ compared to the leading term, as

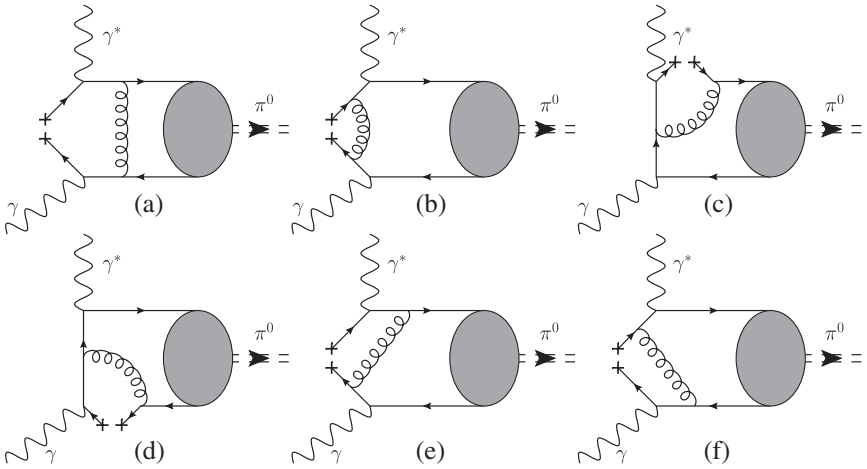

FIG. 4. Factorizable twist-six corrections to the $F_{\gamma^*\gamma\to\pi^0}(Q^2)$ form factor.

expected from dimension (twist) counting. On the other hand, the real photon limit $q^2 \to 0$ of (44) cannot be taken in a straightforward way since the pole at $q^2 = 0$ is clearly unphysical. This singularity appears, obviously, because the quark interacting with the soft photon comes close to the mass shell. Thus the distance it travels becomes large and the OPE cannot be applied. In the full theory, this singularity will be tamed by nonperturbative corrections corresponding to photon emission from large distances, as shown in Fig. 1(b). In the simplest approach, known as vector meson dominance approximation (in the LCSR method, in addition, the continuum contribution is taken into account), nonperturbative corrections amount to a replacement $1/q^2 \to 1/(m_\rho^2 + q^2)$ so that, for $q^2 \to 0$, the singular factor $1/q^2$ is replaced by $1/m_\rho^2$. One obtains

$$F^{\text{Fig.4a}}_{\gamma^*\gamma\to\pi^0}(Q^2) \simeq \frac{\sqrt{2}f_\pi}{3}\frac{32\pi\alpha_s\langle\bar{q}q\rangle^2}{9f_\pi^2 m_\rho^2 Q^4}\int_0^1 dx \frac{\phi^p_{3;\pi}(x)}{x + \bar{x}m_\rho^2/Q^2}. \tag{46}$$

Note that this is a $1/Q^4$ correction to the form factor, not $1/Q^6$ as for equal virtualities. The factor $1/m_\rho^2$ can be identified with the magnetic susceptibility of the quark condensate (in the vector meson dominance approximation) [49,55,64–66]:

$$\chi \simeq \frac{2}{m_\rho^2} \simeq 3.3\ \text{GeV}^{-2}, \tag{47}$$

which enters the definition of the leading twist DA of a real photon [49,55] so that this contribution can be rewritten as a convolution of photon and pion DAs with the coefficient function corresponding to a hard gluon exchange, cf. Fig. 1(b). The direct calculation of this contribution gives

$$F^{\text{Fig.1b}}_{\gamma^*\gamma\to\pi^0}(Q^2) = \frac{\sqrt{2}f_\pi}{3}\frac{16\pi\alpha_s\chi\langle\bar{q}q\rangle^2}{9f_\pi^2 Q^4}\int_0^1 dx\frac{\phi^p_{3;\pi}(x)}{x} \times \int_0^1 dy \frac{\phi_\gamma(y)}{\bar{y}^2}, \tag{48}$$

where $\phi_\gamma(y) \simeq 6y(1-y)$ is the leading twist photon DA [49,55]. The integrals over the quark momentum fractions in (48) are both logarithmically divergent at the end points $x \to 0$, $y \to 1$, which signals that there is an overlap with the soft region, Fig. 1(c).

Another twist-six contribution comes from the diagram in Fig. 4(b):

$$F^{\text{Fig.4b}}_{\gamma^*\gamma\to\pi^0}(Q^2, q^2) = \frac{\sqrt{2}f_\pi}{3}\frac{64\pi\alpha_s\langle\bar{q}q\rangle^2}{27f_\pi^2}\int_0^1 \frac{dx\phi^\sigma_{3;\pi}(x)}{(xQ^2 + \bar{x}q^2)^3}, \tag{49}$$

where the DA $\phi^\sigma_{3;\pi}(x)$ is defined as

$$\langle 0|\bar{q}(0)\sigma_{\mu\nu}\gamma_5 q(\alpha n)|\pi(p)\rangle = \frac{i}{6}(p_\mu x_\nu - p_\nu x_\mu)\frac{f_\pi m_\pi^2}{m_u + m_d} \times \int_0^1 dx e^{-ix\alpha pn}\phi^\sigma_{3;\pi}(x). \tag{50}$$

In the considered approximation (neglecting the quark-antiquark-gluon DAs), the asymptotic form $\phi^\sigma_{3;\pi}(x) = 6x(1-x)$ must be taken [38,61,62]. Note that this contribution is also of the order of $1/Q^4$ and not $1/Q^6$ as suggested by the naïve power counting, since the limit $q^2 \to 0$ leads to a quadratic divergence $\int dx/x^2$ at small momentum fractions. As above, this divergence is regulated in the LCSR approach by correcting the spectral density to include the $\rho(\omega)$-resonance and the continuum.

Next, the diagrams in Figs. 4(c) and 4(d) can be calculated using the light cone expansion of the quark propagator in a background gluon field [67] and picking up terms containing covariant derivatives of the gluon field strength $D^\mu G_{\mu\nu}$. These can be reduced to a quark-antiquark pair via equations of motion. We have checked that there are no terms with additional derivatives compared to the expression given in [67] contributing at the required twist-six level. A straightforward albeit rather lengthy calculation gives

$$F^{\text{Fig.4c,d}}_{\gamma^*\gamma^*\to\pi^0}(Q^2, q^2) = -\frac{\sqrt{2}f_\pi}{3}\frac{16\pi\alpha_s\langle\bar{q}q\rangle^2}{27f_\pi^2} \times \int_0^1 dv(v-\bar{v})v\int_0^1 du\frac{u-v}{\bar{u}} \times \phi^\sigma_{3;\pi}(u)\Big\{\frac{1}{[uvq^2 + (1-uv)Q^2]^3} + \frac{1}{[(1-uv)q^2 + uvQ^2]^3}\Big\}, \tag{51}$$

where it was used that to our accuracy the following relations hold:

$$\frac{x}{2}\left(\phi^p_{3;\pi}(x) + \frac{1}{6}\frac{d\phi^\sigma_{3;\pi}(x)}{dx}\right) = \frac{1}{6}\phi^\sigma_{3;\pi}(x), \qquad \frac{\bar{x}}{2}\left(\phi^p_{3;\pi}(x) - \frac{1}{6}\frac{d\phi^\sigma_{3;\pi}(x)}{dx}\right) = \frac{1}{6}\phi^\sigma_{3;\pi}(x). \tag{52}$$

Finally, the diagrams in Figs. 4(e) and 4(f) vanish. This is in contrast to the similar calculation for the pion electromagnetic form factor in Ref. [42], where only these diagrams contributed.

E. The complete sum rule

Collecting all contributions, we present here the complete light cone sum rule with twist-six accuracy, which will be used in numerical analysis in the next section.

The sum rule for the $\pi^0\gamma^*\gamma$ form factor can be written in terms of the full QCD spectral density $\rho(Q^2, s)$ as

$$F_{\gamma^*\gamma\to\pi^0}(Q^2) = \frac{\sqrt{2}f_\pi}{3}\Big[\int_{s_0}^{\infty}\frac{ds}{s}\rho(Q^2,s) + \frac{1}{m_\rho^2} \times \int_0^{s_0} ds\rho(Q^2,s)e^{(m_\rho^2-s)/M^2}\Big] \equiv F^{\rm hard}_{\gamma^*\gamma\to\pi^0}(Q^2) + F^{\rm soft}_{\gamma^*\gamma\to\pi^0}(Q^2). \quad (53)$$

Here we define the hard and the soft contributions as coming from large $s > s_0$ and small $s < s_0$ invariant masses in the dispersion integral, respectively. Note that the hard part is model-independent whereas the soft part is obtained under the assumption that the contribution of small invariant masses can be represented by a single narrow resonance. The continuum threshold s_0 can be viewed as the separation scale between hard and soft contributions; the dependence on s_0 has to cancel in the sum.

The QCD spectral density can, in turn, be calculated as a sum of contributions of different twists, $t = 2, 4, 6$:

$$\rho(Q^2,s) = \rho^{(2)}(Q^2,s) + \rho^{(4)}(Q^2,s) + \rho^{(6)}(Q^2,s) + \ldots. \quad (54)$$

The leading twist spectral density to the NLO accuracy is given by

$$\rho^{(2)}(Q^2,s) = \frac{x}{Q^2}\sum_{n=0,2\ldots}^{\infty} a_n(\mu)\Big\{\varphi_n(x) + \frac{C_F\alpha_s(\mu)}{4\pi} \times \Big[R_n(Q^2,s)\varphi_n(x) + \tilde\gamma_n^0\sum_{k=0,1\ldots}^{n} H_n^k\varphi_k(x) + 2\sum_{k=0,2\ldots}^{n} G_n^k\varphi_k(x) - 3\tilde\gamma_n^0\bar x\Big]\Big\}, \quad (55)$$

where

$$R_n(Q^2,s) = -3[1 + 2(\psi(2) - \psi(2+n)] + \frac{\pi^2}{3} - \ln^2\Big(\frac{\bar x}{x}\Big) - \tilde\gamma_n^{(0)}\ln\Big(\frac{s}{\mu^2}\Big). \quad (56)$$

The integrals corresponding to the hard part, $s > s_0$ in Eq. (53), can be taken analytically. The corresponding expression in Eq. (E.17) in [20] contains a misprint: The term $-3\ln^2(s_0/u)$ has to be replaced by $-3\ln(s_0/u)$.

The twist-four spectral density is equal to

$$\rho^{(4)}(Q^2,s) = \frac{160}{3Q^4}\delta_\pi^2(\mu)x^3\bar x(1-2x). \quad (57)$$

Finally, the twist-six contribution can be written as

$$\rho^{(6)}(Q^2,s) = 8\pi C_F\alpha_s(\mu)\frac{\langle\bar qq\rangle^2}{N_c f_\pi^2}\frac{x^2}{Q^6}\Big[2x\log x + 2x\log\bar x - x + 2\delta(\bar x) - \frac{1}{\bar x} + \delta(\bar x)\int_0^1\frac{dx'}{\bar x'}\Big]. \quad (58)$$

Note that the last two terms combine to a "plus" distribution, $1/[1-x]_+$. In all expressions (55)–(58), $x \equiv Q^2/(Q^2+s)$.

We want to emphasize that the twist-six contribution is not suppressed compared to the twist-four one by an extra power of Q^2, and the same is true for all higher-twist corrections. The twist expansion in LCSRs goes in powers of $\Lambda^2_{\rm QCD}/s_0$, $\Lambda^2_{\rm QCD}/M^2$, where $\Lambda^2_{\rm QCD}$ is a generic dimensionful parameter that characterizes the size of higher-twist matrix elements.

IV. NUMERICAL ANALYSIS

A. The parameters

All numerical results in this work are obtained using the two-loop running QCD coupling with $\Lambda^{(4)}_{\rm QCD} = 326$ MeV and $n_f = 4$ active flavors. Unless stated otherwise, all nonperturbative parameters and models of the pion DA refer to the renormalization scale $\mu_0 = 1$ GeV; $\alpha_s(\mu_0) = 0.494$.

A natural factorization and renormalization scale μ in the calculation of the $\pi^0\gamma^*\gamma^*$ form factor with two large virtualities is given by the virtuality of the quark propagator $\mu^2 \sim xQ^2 + \bar xq^2$ and depends on the quark momentum fraction. If $q^2 \to 0$, in the LCSR framework the relevant factorization scale becomes $\mu^2 \sim xQ^2 + \bar xM^2$, or $\mu^2 \sim xQ^2 + \bar x s_0$ for large values of the Borel parameter, see e.g. [42]. Note that in the first integral in (53) the quark virtuality is never large, of order Q^2: The restriction $s < s_0$ translates to $\bar x < s_0/(s_0+Q^2)$ and hence $\mu^2 \simeq 2s_0$ as $Q^2 \to \infty$, in agreement with the interpretation of this term as the soft contribution. Numerical calculations with the x-dependent factorization scale are rather slow, so in this work we use a fixed scale, replacing x by the constant $\langle x\rangle$ which is varied within a certain range:

$$\mu^2 = \langle x\rangle Q^2 + \langle\bar x\rangle s_0, \qquad 1/4 < \langle x\rangle < 3/4. \quad (59)$$

The choice of the Borel parameter in LCSRs is discussed in [54,68]. The subtlety is that the twist expansion in LCSRs goes in powers of $1/(xM^2)$, rather than $1/M^2$ in the classical Shifman-Vainshtein-Zakharov approach. Hence one has to use somewhat larger values of M^2 compared to the QCD sum rules for two-point correlation functions in order to ensure the same hierarchy of contributions. We choose as the "working window"

$$1 < M^2 < 2\ {\rm GeV}^2 \quad (60)$$

and $M^2 = 1.5\ {\rm GeV}^2$ as the default value in our calculations.

We use the standard value $s_0 = 1.5$ GeV^2 for the continuum threshold as the central value, and the range

$$1.3 < s_0 < 1.7 \text{ GeV}^2 \tag{61}$$

in the error estimates. We did not attempt to consider corrections due to the finite width of the ρ, ω resonances. The estimates in Ref. [14] suggest that such corrections may result in the enhancement of the form factor by 2–4% in the small-to-mediate Q^2 region where the resonance part dominates. We believe that such uncertainties are effectively covered by our (conservative) choice of the continuum threshold.

Finally, we use the values $\delta_\pi^2 = 0.2 \pm 0.4$ GeV^2 and $\langle \bar{q}q \rangle = -(240 \pm 10 \text{ MeV})^3$ (at the scale 1 GeV) for the normalization parameter for twist-four DAs (43) and the quark condensate, respectively.

B. Testing simple models

We start our analysis with the comparison of the LCSR predictions for the $\pi^0\gamma^*\gamma$ form factor for three simple models of the pion DA that are often quoted in the literature:

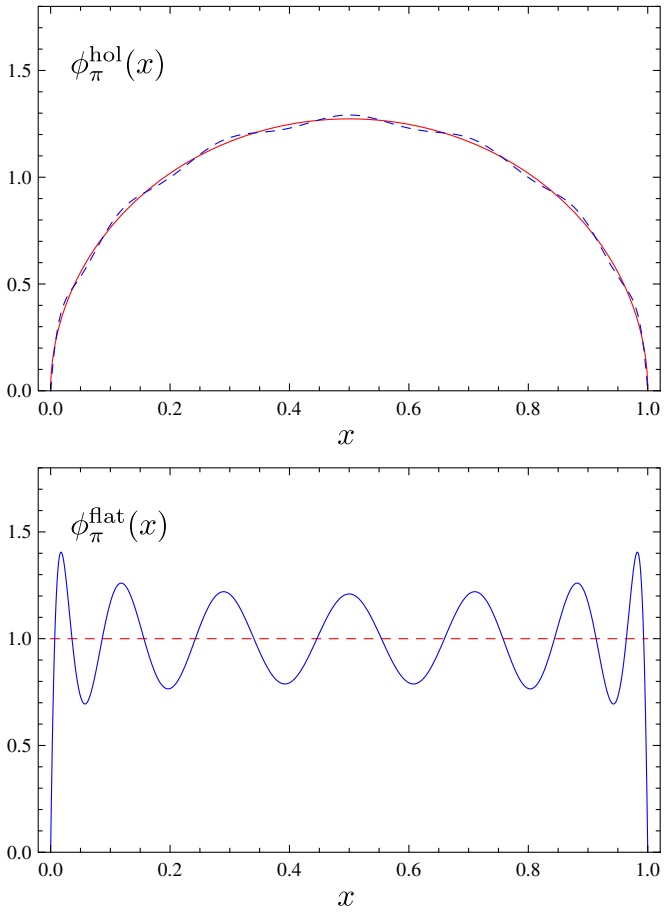

FIG. 5 (color online). The $n = 12$ truncations (63) of the pion DAs $\phi_\pi^{\rm hol}(x)$ [dashed (blue) line] and $\phi_\pi^{\rm flat}(x)$ [(blue) curve] compared to the exact expressions [(red) curve and (red) dashed line, respectively].

$$\phi_\pi^{\rm as}(x) = 6x(1-x), \qquad \phi_\pi^{\rm hol}(x) = \frac{8}{\pi}\sqrt{x(1-x)},$$
$$\phi_\pi^{\rm flat}(x) = 1. \tag{62}$$

The asymptotic $\phi_\pi^{\rm as}(x)$ and flat $\phi_\pi^{\rm flat}(x)$ DAs have already been discussed above; the "holographic" model $\phi_\pi^{\rm hol}(x)$ is inspired by the anti–de Sitter/QCD correspondence [69] (see, however, [70]).

Apart from the general interest, considering these models allows one to test the applicability of the Gegenbauer expansion. To this end, consider the approximations to $\phi_\pi^{\rm flat}(x)$, $\phi_\pi^{\rm hol}(x)$ by the truncated series at order n:

$$\phi_\pi^{\rm flat(hol),(n)}(x) = \sum_{k=0,2,\ldots}^{n} a_k^{\rm flat(hol)} \varphi_k(x), \tag{63}$$

where

$$a_k^{\rm hol} = \frac{2n+3}{3\pi}\left(\frac{\Gamma[(n+1)/2]}{\Gamma[(n+4)/2]}\right)^2, \tag{64}$$

and $a_k^{\rm flat}$ are given in Eq. (15).

The expressions collected in Sec. III and Appendixes A and B allow us to construct the sum rules using up to seven terms $k = 0, 2, \ldots, 12$ corresponding to the $n = 12$ truncation. The resulting DAs $\phi_\pi^{\rm flat,(n=12)}(x)$, $\phi_\pi^{\rm hol,(n=12)}(x)$ are compared with the exact ones, $\phi_\pi^{\rm flat}(x)$, $\phi_\pi^{\rm hol}(x)$, in Fig. 5. Note that the $n = 12$ approximation is very good for the holographic DA, whereas, for the flat one, the convergence is slow and there are large oscillations.

Next, we use the three DAs in Eq. (62) (the last two ones truncated at order $n = 12$) to calculate the $\pi^0\gamma^*\gamma$ form factor. The results are shown in Fig. 6.

One sees that both the asymptotic and the holographic models fail to describe the *BABAR* data [10]. The flat DA fares better for the largest Q^2 values, but it is considerably

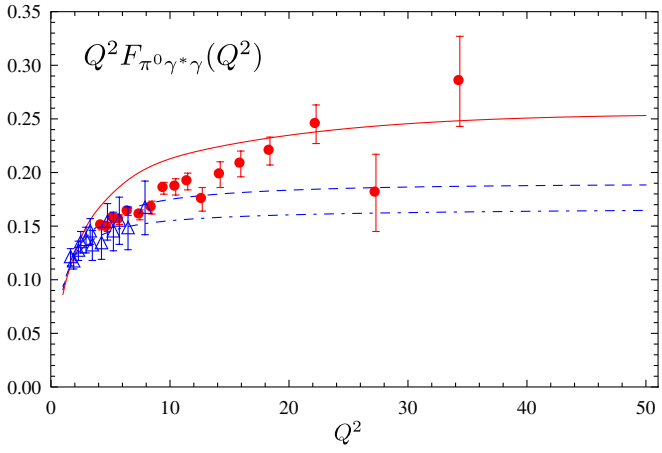

FIG. 6 (color online). The pion transition form factor for the flat [solid (red) line], holographic [dashed (blue) line] and asymptotic [dash-dotted (blue) line] models for the pion DA, cf. Eq. (62). The experimental data are from [10] (full circles) and [8] (open triangles).

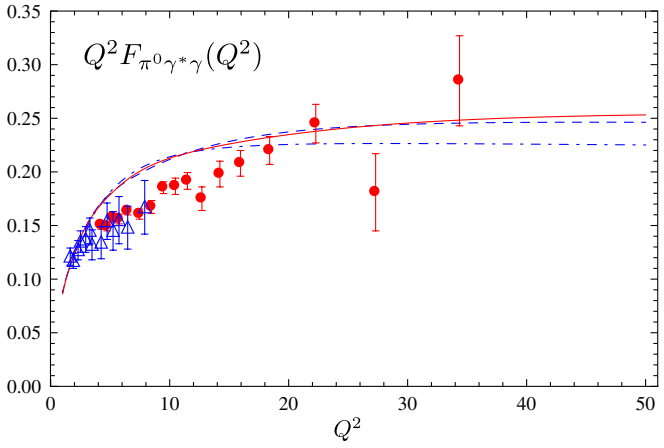

FIG. 7 (color online). The pion transition form factor for three different approximations for the flat DA: $n = 12$ [solid (red) line], $n = 8$ [dashed (blue) line], and $n = 4$ [dash-dotted (blue) line]. The experimental data are from [10] (full circles) and [8] (open triangles).

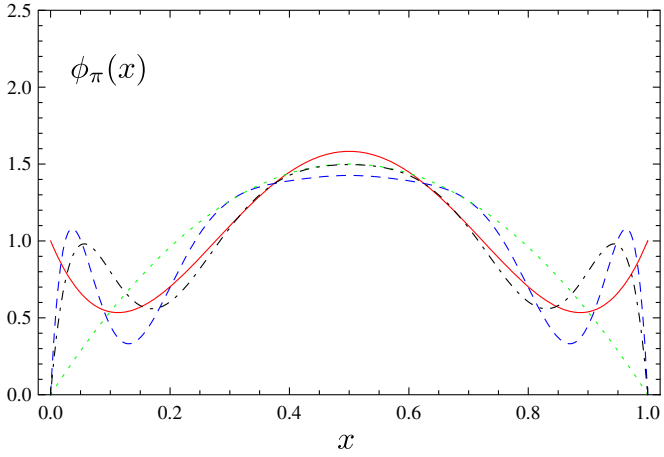

FIG. 8 (color online). Model I, [solid (red) curve], model II [dashed (blue) curve], and model III [dash-dotted (black) curve] of the pion DA at the scale 1 GeV. The asymptotic pion DA is shown by the (green) dots for comparison.

above the experiment at intermediate $Q^2 \sim 5 - 15$ GeV^2. In order to understand this behavior, we compare in Fig. 7 the predictions for three different truncations of the flat DA: $\phi_\pi^{\text{flat},(n=12)}(x)$, $\phi_\pi^{\text{flat},(n=8)}(x)$, and $\phi_\pi^{\text{flat},(n=4)}(x)$.

We observe that all three calculations are very close to each other for $Q^2 \leq 18$ GeV^2 so that in this region contributions of Gegenbauer polynomials starting with $n = 6$–8 play no role. This conclusion is in agreement with our discussion of the MR model in Sec. II and also supports the usual procedure of modeling the pion DA by the asymptotic expression and contributions of first two Gegenbauer polynomials in applications to B-decays and pion electromagnetic form factor, e.g. [14,17–22]. We also see that contributions of the Gegenbauer polynomials $n = 6, 8$ become significant for the momentum transfers $Q^2 > 18$ GeV^2. In the region $Q^2 > 30$ GeV^2, higher-order polynomials should be included into analysis as well, but the accuracy of the existing experimental data is not sufficient to draw definite conclusions.

In other words, the differences between the predictions of asymptotic, holographic, and flat DAs in Fig. 6 for $Q^2 < 20$ GeV^2 are mostly due to the different values of the coefficients a_2 and a_4, with a_6 also playing some role. This leaves us with two to three parameters that can be tuned to attempt a better description of the *BABAR* data, the task that we address now.

C. Confronting the *BABAR* data

The extraction of the pion DA with meaningful error estimates requires a global fit to the pion transition and electromagnetic form factor, weak $B(D) \to \pi\ell\nu$ decays, and the couplings $g_{\pi NN}$, $g_{BB^*\pi}$ etc. using a Monte Carlo scan of the space of all available parameters, which goes beyond the tasks of this work. Fitting of the *BABAR* data is not attempted. Instead, we present results for three sample models that describe the $\pi^0\gamma^*\gamma$ form factor sufficiently well and discuss their general features.

The three models that we consider below are shown in Fig. 8 (at the scale 1 GeV), and the corresponding Gegenbauer coefficients are collected in Table II.

The first model

$$\phi_\pi^{\text{I}}(x) = 1 - (7/18 - 0.13)\varphi_2(x) \tag{65}$$

is nothing but the flat DA with the reduced second Gegenbauer coefficient, $a_2^{\text{flat}} \to 0.130$.

It has a long "tail" of higher-order Gegenbauer polynomials. From the previous discussion we expect that this

TABLE II. Gegenbauer coefficients of three sample models of pion DA that are consistent with *BABAR* measurements [10] of the transition form factor; cf. Fig. 9.

Model	Scale	a_2	a_4	a_6	a_8	a_{10}	a_{12}
I	$\mu = 1$ GeV	0.130	0.244	0.179	0.141	0.116	0.099
	$\mu = 2$ GeV	0.089	0.148	0.097	0.070	0.054	0.044
II	$\mu = 1$ GeV	0.140	0.230	0.180	0.05	0.0	0.0
	$\mu = 2$ GeV	0.096	0.140	0.098	0.024	-0.001	$<10^{-3}$
III	$\mu = 1$ GeV	0.160	0.220	0.080	0.0	0.0	0.0
	$\mu = 2$ GeV	0.110	0.133	0.043	-0.001	$<10^{-3}$	$<10^{-3}$

tail actually gives no contribution in the Q^2 range of interest. In order to check that this is indeed the case, we consider the second model in which the higher-order coefficients a_{10}, a_{12} are put to zero at the reference scale 1 GeV, and we keep a small a_8 to avoid an oscillating behavior at $x \sim 1/2$. Note that nonzero values of the coefficients a_{10}, a_{12} (and all higher) are generated at higher scales, but this mixing is numerically insignificant. Finally, the third model is chosen to explore the sensitivity of the predictions to particular values of a_2, a_4 and a_6, and to see whether they are correlated.

The calculations using these models are compared with the available experimental data in Fig. 9. The results are shown by thick solid curves: The line thickness shows the uncertainty and is calculated as a square root of the sum of squares of the error bars on the LCSR predictions due to variation of the parameters within the limits specified in Sec. IV A. These include the factorization scale dependence, dependence on the Borel parameter M^2, and the continuum threshold s_0, and on higher-twist parameters δ_π^2 and $\langle \bar{q}q \rangle$.

The distinctive feature of all three models is the large value of the fourth Gegenbauer moment, a_4, which is necessary in order to accommodate the observed rise of the scaled form factor in the $Q^2 = 5$–20 GeV^2 range. It is not possible to trade the large value of a_4 for the increased a_2 or a_6, although of course there is some correlation.

Our value of $a_2 \sim 0.13$–0.16 at 1 GeV is at the low end of the existing estimates, cf. Table I, and, in particular, it is lower compared to the earlier LCSR analysis of the transition form factor in Refs. [14,20,22]. The main reason for this difference is that the Borel parameter in [14,20] is fixed at an *ad hoc* value $M^2 = 0.7$ GeV^2, whereas in the present analysis we allow its variation in the 1–2 GeV^2 range. For the specific choice $a_2(\mu_{\rm SY}) = 0.14$, $a_4(\mu_{\rm SY}) = -0.09$, $\mu_{\rm SY} \simeq 2.4$ GeV, advocated in [14,20], the result for the form factor at $Q^2 = 5$ GeV^2 is increased by $\sim$11% if M^2 is changed from 0.7 to 1.5 GeV^2. Another reason is that in [14,20,22] the twist-six correction is not included. The size of this correction depends strongly on the Borel parameter. For our choice, $M^2 \sim 1.5 \pm 0.5$ GeV^2, the twist-six term proves to be small: factor three smaller that the twist-four correction (see below), which is gratifying as it signals convergence of the OPE. In contrast, at $M^2 = 0.7$ GeV^2, the twist-six correction is almost of the same size as twist-four and has opposite sign. Hence it must be included. In both cases (increasing the Borel parameter and/or including the twist-six correction), the net effect is the increase of the form factor by 5–10% in the CLEO range which has to be compensated by a smaller value of the second Gegenbauer moment.

The error band indicated by thickness of the curves in Fig. 9 has to be taken with caution. A weak scale dependence of our results is largely due to strong cancellations of the NLO radiative corrections between the contributions of

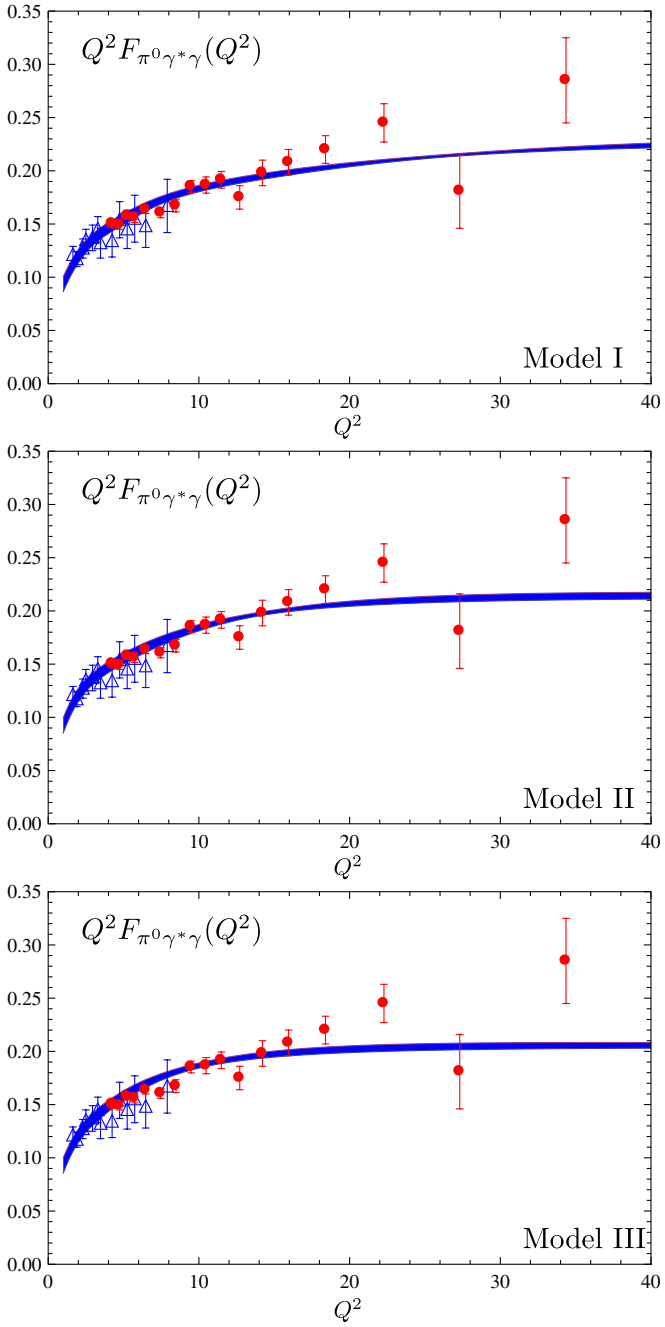

FIG. 9 (color online). The pion transition form factor for the three models of the pion DA specified in the text. The experimental data are from [10] (full circles) and [8] (open triangles).

the asymptotic DA and higher Gegenbauer polynomials and may not be representative for the size of NNLO corrections which are only known in the $\overline{\rm CS}$ factorization scheme; see [33] for a detailed discussion of the related ambiguities. Also, the uncertainty in the twist-four contribution is not reduced to the δ_π^2 parameter: Using an alternative, renormalon model [71] of the twist-four pion DA generally produces somewhat larger corrections. We have checked that the difference is not very significant, however,

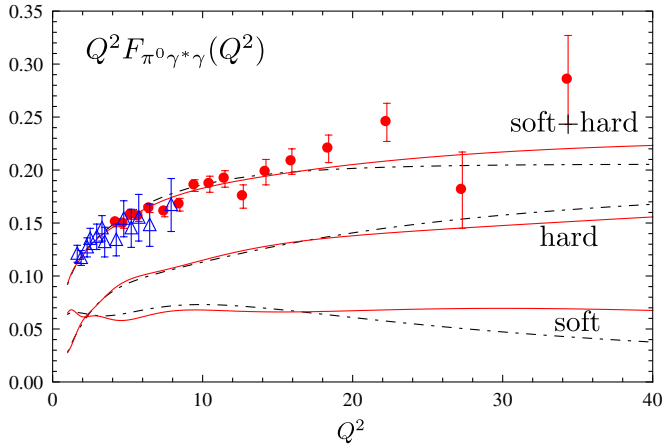

FIG. 10 (color online). Contributions to the $\pi^0\gamma^*\gamma$ form factor from large (hard) and small (soft) invariant masses in the dispersion representation, cf. Eq. (53), for model I (solid curves) and model III (dash-dotted curves). The experimental data are from [10] (full circles) and [8] (open triangles).

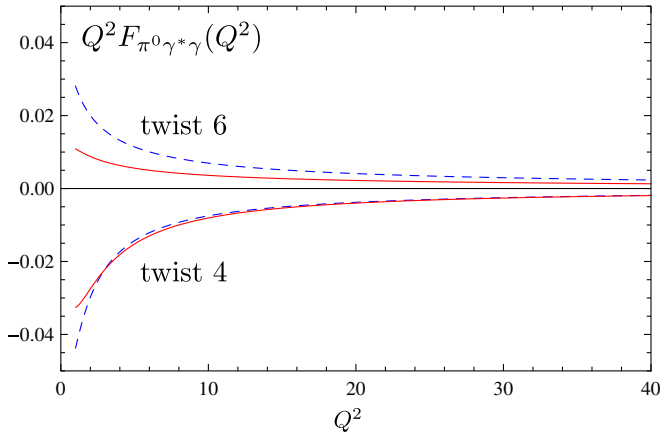

FIG. 11 (color online). Higher-twist contributions to the $\pi^0\gamma^*\gamma$ form factor for the values of the Borel parameter $M^2 = 1.5$ (solid curves) and $M^2 = 0.7$ GeV^2 (dashed curves).

and does not affect any of our conclusions. Hence we do not show the corresponding results.

The hard and soft contributions to the $\pi^0\gamma^*\gamma$ form factor as defined in Eq. (53) are shown separately for model I (solid curves) and model III (dash-dotted curves) in Fig. 10.

Asymptotically, for $Q^2 \to \infty$, the soft contribution is power-suppressed compared to the hard one, $\sim s_0/Q^2$. This suppression sets in for very large values of Q^2, however, especially if the pion DA is enhanced close to the end points. For example, for our model III, the soft contribution still accounts for circa 25% of the form factor at $Q^2 = 30$ GeV^2 (for the separation scale $s_0 = 1.5$ GeV^2). This means that a purely perturbative leading twist QCD calculation of the transition form factor for one real photon in collinear factorization should not be expected to have high accuracy. A lattice calculation of the transition $\pi\rho\gamma^*$ form factor at $Q^2 \sim 2$–5 GeV^2 would help to estimate the contribution of the resonance region more reliably.

Finally, in Fig. 11 we show the higher-twist contributions. The twist-four correction is negative and the twist-six one is positive. It turns out that the twist-six contribution depends rather strongly on the Borel parameter. It is suppressed in the Q^2 region of interest relative to the twist-four term for our choice $M^2 = 1.5$ GeV^2, but it increases rapidly for smaller M^2. For example, for $M^2 = 0.7$ GeV^2 used in [14,20], the twist-six correction is ~ 0.6 of the twist-four term at $Q^2 = 1$ GeV^2, becomes equal (with opposite sign) at $Q^2 \simeq 14$ GeV^2, and overshoots twist-four for larger Q^2 (because it contains a logarithmic $\sim \ln Q^2$ enhancement).

D. Other processes

The pion DA is a universal function and, if extracted from one reaction, should, in general, describe all exclusive or semi-inclusive processes that involve a pion in the initial and/or final states. The most prominent of them are the pion electromagnetic form factor and the weak semileptonic decay rate $B \to \pi\ell\nu_\ell$. Without going in detail, we present here the corresponding LCSR calculations using the pion DA models as specified above.

The LCSRs for the pion electromagnetic form factor were derived in Refs. [42,43,72] and later explored also in [44,73]. These sum rules are known to the same accuracy as for the transition form factor, i.e. including the NLO perturbative contribution and twist-four and twist-six corrections. Explicit expressions can be found in [43].

The results are shown in Fig. 12 in comparison with the experimental data [74,75]. For this plot we have chosen $M^2 = 1.5$ GeV^2, $s_0^\pi = 0.8$ GeV^2 and the factorization scale $\mu = (1/2)(Q^2 + s_0)$ as representative values; the three curves correspond to the models of the pion DA in Fig. 8.

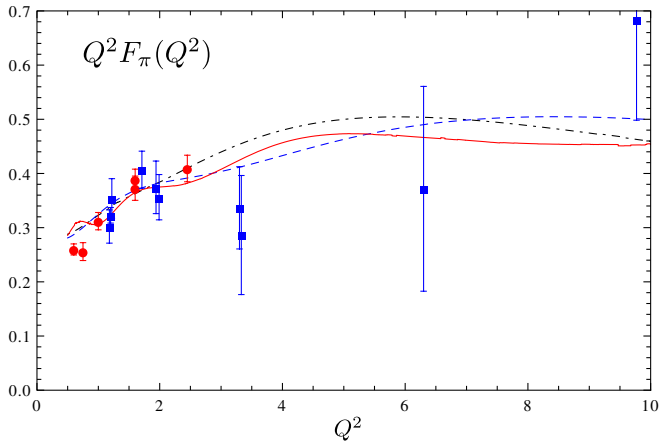

FIG. 12 (color online). Electromagnetic pion form factor for the three models of pion DA described in the text. Identification of the curves follows Fig. 8. The experimental data are from [74] (blue squares) and [75] (red circles).

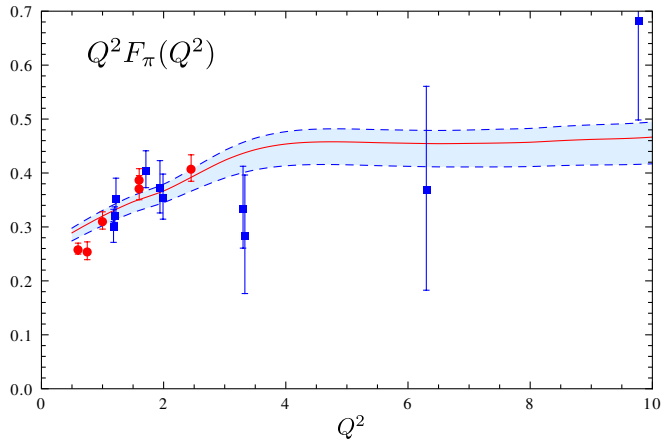

FIG. 13 (color online). Electromagnetic pion form factor for model I (with reduced $a_{12} = 0.099 \to 0.04$). The solid curve, upper dashed curve, and lower dashed curve are calculated using the Borel parameters $M^2 = 1.5$, $M^2 = 2$, and $M^2 = 1$ GeV^2, respectively. The experimental data are from [74] (blue squares) and [75] (red circles).

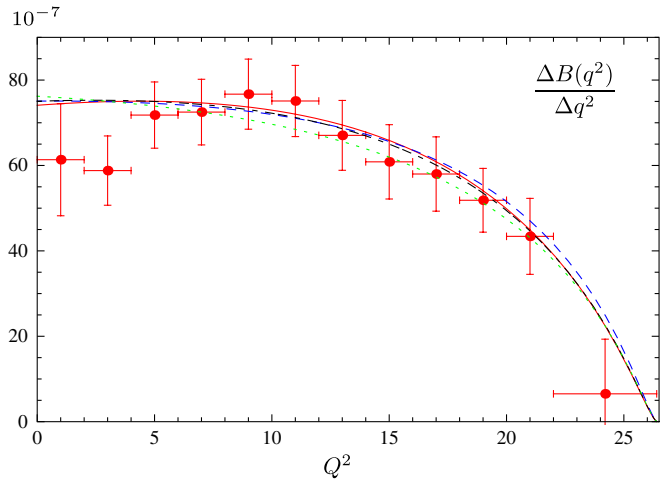

FIG. 14 (color online). The differential $\pi^- e^+ \nu_e$ decay width. Experimental data are taken from [78]. A two-parameter Bourrely-Caprini-Lellouch fit [76] is applied to the sum rule calculation to extrapolate it to the whole q^2 range. For normalization, we assume $|Vub| = 3.6x10^{-3}$. The identification of the curves follows Fig. 8; see also text.

The agreement is very good. Note that the oscillations at small Q^2 in model I are an artifact of the truncation of the Gegenbauer expansion. They can be removed, e.g. by reducing $a_{12}^{\rm flat} = 0.099 \to 0.04$, which has the effect of smoothening the DA, especially in the central region.

It has to be mentioned that the pion electromagnetic form factor is much more affected by soft contributions compared to the transition form factor and hence is also more model dependent. In particular, the Borel parameter dependence is much stronger; see Fig. 13, where the calculations using $M^2 = 1$ and $M^2 = 2$ GeV^2 are shown by dashed curves for comparison.

The weak decay $B \to \pi \ell \nu_\ell$ has received a lot of attention as one of the primary sources of information on the weak mixing angle $|V_{ub}|$ in the standard model. The differential decay width dB/dq^2, where q^2 is the invariant mass of the leptons, is given by the square of the $B \to \pi$ form factor, modulo relevant Cabibbo-Kobayashi-Maskawa angles and kinematic factors:

$$\frac{dB}{dq^2}(B \to \pi^- e^+ \nu_e) = \frac{G_F^2 |V_{ub}|^2}{192\pi^3 m_B^3} \tau_B \lambda^{3/2}(q^2) |f_{B\pi}^+(q^2)|^2. \tag{66}$$

In this equation $\lambda(q^2) = (m_B^2 + m_\pi^2 - q^2)^2 - 4m_B^2 m_\pi^2$, and τ_B is the mean lifetime of the B-meson. Below we use $|V_{ub}| = 3.6 \times 10^{-3}$ to fix the overall normalization.

LCSRs enable one to calculate the form factor up to $q^2 = 14$ GeV^2, and a two-parameter Bourrely-Caprini-Lellouch [76] fit is then used to extrapolate the calculation to the whole kinematic region $0 \le q^2 \le 26.4$ GeV^2. The latest and most advanced LCSR calculations of this form factor [46,77] include NLO corrections in leading twist and also for a part of the twist-three contributions. Twist-four corrections are taken into account in the leading order. In the calculations presented in Fig. 14, we use the central values of the sum rule parameters from Ref. [46].

All our models of pion DA describe the data [78] reasonably well and are nearly indistinguishable in the $q^2 < 14$ GeV^2 range where the direct sum rule calculation is applicable. The calculation using "conventional" pion DA with $a_2 = 0.17$ and $a_4 = 0.06$ (at 1 GeV) [46] is shown by green dots in Fig. 8 for comparison. We conclude that the $B \to \pi$ form factor is not very sensitive to the higher Gegenbauer moments beyond a_2; a low value $a_2 < 0.2$ (at 1 GeV) is preferred.

The value of the pion DA in the middle point in all our models is close to the asymptotic value $\phi_\pi(x = 1/2) = 1.5$. This number is within the range in Eq. (13) and somewhat larger than it was assumed in the LCSR calculations of pion-hadron couplings [50,56–60]. The larger value is in fact welcome and can reduce the well-known ~30% discrepancy of the sum rule calculation [56,57] of $g_{D^*D\pi}$ with the experiment.

V. SUMMARY AND CONCLUSIONS

The recent *BABAR* measurement [10] of the pion transition form factor provided the most direct evidence so far that the pion distribution amplitude deviates considerably from its asymptotic form. This result has to be considered as a success of an early QCD prediction [35] of a broad pion DA at a low scale, but it also created a lot of excitement because a significant scaling violation at $Q^2 > 5$–10 GeV^2 came out unexpectedly.

The main lesson to be learned from the *BABAR* data is that attempts to describe the transition form factor with one real photon entirely in the framework of perturbative QCD

are futile; nonperturbative soft corrections must be taken into account.

We have adopted the LCSR approach [49–51], which has the advantage that it is applicable to a broad class of reactions and has been thoroughly tested. In this work we go beyond the existing analysis [14,17–22] in two aspects. First, we calculate a new, twist-six contribution to LCSRs which proves to be sizeable. Second, we extend the existing formalism to allow for the contributions of higher-order Gegenbauer polynomials, which allows one to consider DAs of arbitrary shape and also address the question of convergence of the Gegenbauer expansion which generated some confusion.

We find that a significant rise of the scaled form factor $Q^2F_{\pi^0\gamma^*\gamma}(Q^2)$ in the $Q^2 = 5$–20 GeV^2 range observed by the *BABAR* Collaboration [10] can be explained by a large value of the fourth Gegenbauer moment

$$a_4 > a_2$$

in the pion DA, leading to models of the type shown in Fig. 8 which are not far from the asymptotic distribution in the central region but have enhancements close to the end points. Our preferred models also include sizeable a_6 coefficients; these can be put to zero at the cost of further increasing a_4, which does not seem to be attractive. The higher partial waves, a_8, a_{10}, etc., contribute only marginally in the *BABAR* Q^2 range, the reason being that contributions of the endpoint regions in the pion DA are cut off by soft effects.

We have checked that the models of pion DA having such an inverse hierarchy, $a_4 > a_2$, give good description of the pion electromagnetic and weak decay $B \to \pi$ form factors calculated within the same LCSR approach. This agreement is not trivial since the size of soft corrections is very different and also the duality assumption of the contribution of small invariant masses is applied in different channels. The small value of $a_2 < 0.2$ (at 1 GeV) was actually suggested before from the fit to the $B \to \pi\ell\nu_\ell$ differential decay width [46], whereas large a_4 does not have a noticeable effect in this case because the effective momentum transfer in B decays is much lower.

The main uncertainty of the LCSR calculation is due to the assumption that contributions of low invariant masses in the dispersion relation in QCD diagrams are dual (i.e. coincide in integral sense) with the contribution of resonances, here, the ρ, ω mesons. The accuracy of duality is difficult to quantify, but it is usually believed to be better than 20% on the experience of many successful applications. An inspection shows that our result $a_4 > a_2$ is related to a rather large value of the transition form factor $F_{\rho\pi\gamma^*}(Q^2)$ in the $Q^2 \sim 2$–5 GeV^2 range that follows from duality. For comparison, this form factor estimated as the integral of the spectral density below $s = 1.5$ GeV^2 in the MR model [23] appears to be a factor 2–3 lower, which explains why in this model the *BABAR* data can be fitted by a CZ-type pion DA with a large a_2 coefficient and $a_4 = 0$. Lattice calculations of the $F_{\rho\pi\gamma^*}(Q^2)$ form factor in a few GeV^2 range and improved accuracy on a_2 would help to discriminate between these two possibilities. More precise experimental data in the $Q^2 = 15$–30 GeV^2 range would, of course, be most welcome as well.

ACKNOWLEDGMENTS

V. M. Braun is grateful to M. Diehl, A. Khodjamirian, P. Kroll, and A. Radyushkin for numerous discussions on the subject of this work, and to N. Stefanis for correspondence concerning the results in Ref. [18]. S. S. Agaev appreciates the warm hospitality that members of the Theoretical Physics Institute extended to him at Regensburg University, where this work has been carried out. The work of S. S. Agaev was supported by DAAD Grant No. A/10/02381.

Note added.—Our conclusion that soft nonperturbative corrections strongly suppress contributions of higher-order Gegenbauer polynomials to the pion DA and thus render the question of the endpoint behavior of the pion DA effectively irrelevant is also supported by an independent study [80] within the k_t-factorization approach.

APPENDIX A: SCALE DEPENDENCE OF THE PION DA

The scale dependence of the coefficients $a_n(\mu)$ in the Gegenbauer expansion of the pion DA is determined by Eq. (9).

The RG factor $E_n^{\rm NLO}(\mu, \mu_0)$ in this expression is given by

TABLE III. The mixing matrix M_n^k (A6).

M_n^k	$k=0$	$k=2$	$k=4$	$k=6$	$k=8$	$k=10$
$n=0$	0					
$n=2$	$-11.23+1.73n_f$	0				
$n=4$	$-1.41+0.56n_f$	$-22.02+1.65n_f$	0			
$n=6$	$0.03+0.26n_f$	$-7.76+0.82n_f$	$-22.77+1.39n_f$	0		
$n=8$	$0.29+0.14n_f$	$-3.34+0.48n_f$	$-10.34+0.84n_f$	$-21.72+1.18n_f$	0	
$n=10$	$0.31+0.09n_f$	$-1.58+0.30n_f$	$-5.46+0.55n_f$	$-11.3+0.79n_f$	$-20.35+1.02n_f$	0
$n=12$	$0.28+0.06n_f$	$-0.78+0.21n_f$	$-3.13+0.38n_f$	$-6.64+0.56n_f$	$-11.54+0.73n_f$	$-19.0+0.9n_f$

$$E_n^{\rm NLO}(\mu,\mu_0)=\left[\frac{\alpha_s(\mu)}{\alpha_s(\mu_0)}\right]^{\gamma_n^{(0)}/2\beta_0}\left\{1+\frac{\alpha_s(\mu)-\alpha_s(\mu_0)}{8\pi}\times\frac{\gamma_n^{(0)}}{\beta_0}\left(\frac{\gamma_n^{(1)}}{\gamma_n^{(0)}}-\frac{\beta_1}{\beta_0}\right)\right\}. \tag{A1}$$

The corresponding LO RG factor $E_n^{\rm LO}(\mu,\mu_0)$ is obtained by keeping only the first term in the braces.

Here $\beta_0(\beta_1)$ and $\gamma_n^{(0)}(\gamma_n^{(1)})$ are the LO (NLO) coefficients of the QCD β-function and the anomalous dimensions, respectively:

$$\mu^2\frac{d\alpha_s(\mu)}{d\mu^2}=\beta(\alpha_s)=-\alpha_s\left\{\beta_0\frac{\alpha_s}{4\pi}+\beta_1\left(\frac{\alpha_s}{4\pi}\right)^2+\ldots\right\},$$
$$\gamma_n(\alpha_s)=-\frac{1}{2}\left\{\gamma_n^{(0)}\frac{\alpha_s}{4\pi}+\gamma_n^{(1)}\left(\frac{\alpha_s}{4\pi}\right)^2+\ldots\right\}. \tag{A2}$$

The first two coefficients of the beta-function are

$$\beta_0=11-\frac{2}{3}n_f,\qquad \beta_1=102-\frac{38}{3}n_f, \tag{A3}$$

whereas $\gamma_n^{(0)}$ is given by

$$\gamma_n^{(0)}=2C_F\left(1-\frac{2}{(n+1)(n+2)}+4\sum_{m=2}^{n+1}\frac{1}{m}\right). \tag{A4}$$

The NLO anomalous dimensions can most easily be obtained using the FEYNCALC MATHEMATICA package [79]. For convenience, we present explicit expressions up to $n=12$ that are used in our calculations ($\gamma_0^{(1)}=0$):

$$\gamma_2^{(1)}=\frac{34450}{243}-\frac{830}{81}n_f,\qquad \gamma_4^{(1)}=\frac{662846}{3375}-\frac{31132}{2025}n_f,$$
$$\gamma_6^{(1)}=\frac{718751707}{3087000}-\frac{3745727}{198450}n_f,$$
$$\gamma_8^{(1)}=\frac{293323294583}{1125211500}-\frac{19247947}{893025}n_f,$$
$$\gamma_{10}^{(1)}=\frac{212204133652373}{748828253250}-\frac{512808781}{21611205}n_f,$$
$$\gamma_{12}^{(1)}=\frac{995653107122188087}{3290351344780500}-\frac{93360116539}{3652293645}n_f.$$

The off-diagonal mixing coefficients d_n^k in Eq. (9) are given by the following expression:

$$d_n^k(\mu,\mu_0)=\frac{M_n^k}{\gamma_n^{(0)}-\gamma_k^{(0)}-2\beta_0}\times\left\{1-\left[\frac{\alpha_s(\mu)}{\alpha_s(\mu_0)}\right]^{[\gamma_n^{(0)}-\gamma_k^{(0)}-2\beta_0]/2\beta_0}\right\}. \tag{A5}$$

The matrix M_n^k is defined as

$$M_n^k=\frac{(k+1)(k+2)(2n+3)}{(n+1)(n+2)}[\gamma_n^{(0)}-\gamma_k^{(0)}]\times\left\{\frac{8C_FA_n^k-\gamma_k^{(0)}-2\beta_0}{(n-k)(n+k+3)}+4C_F\frac{A_n^k-\psi(n+2)+\psi(1)}{(k+1)(k+2)}\right\}, \tag{A6}$$

where

$$A_n^k=\psi\left(\frac{n+k+4}{2}\right)-\psi\left(\frac{n-k}{2}\right)+2\psi(n-k)-\psi(n+2)-\psi(1). \tag{A7}$$

For convenience, we have collected numerical values of the coefficients M_n^k for $n\le 12$ in Table III.

TABLE IV. Numerical values of the coefficients G_n^k (33).

G_n^k	$k=0$	$k=2$	$k=4$	$k=6$	$k=8$	$k=10$	$k=12$
$n=0$	-1						
$n=2$	$\frac{3}{2}$	$-\frac{35}{12}$					
$n=4$	$\frac{3}{4}$	$\frac{161}{72}$	$-\frac{203}{45}$				
$n=6$	$\frac{83}{180}$	$\frac{49}{40}$	$\frac{781}{300}$	$-\frac{29531}{5040}$			
$n=8$	$\frac{177}{560}$	$\frac{4}{5}$	$\frac{6259}{4200}$	$\frac{4437}{1568}$	$-\frac{177133}{25200}$		
$n=10$	$\frac{487}{2100}$	$\frac{6181}{10800}$	$\frac{7601}{7560}$	$\frac{7823}{4704}$	$\frac{338561}{113400}$	$-\frac{1676701}{207900}$	
$n=12$	$\frac{74141}{415800}$	$\frac{17167}{39600}$	$\frac{697}{945}$	$\frac{177799}{155232}$	$\frac{2227921}{1247400}$	$\frac{5672237}{1829520}$	$-\frac{30946717}{3439800}$

TABLE V. Numerical values of the coefficients H_n^k (34).

H_n^k	$k=0$	$k=1$	$k=2$	$k=3$	$k=4$	$k=5$	$k=6$	$k=7$	$k=8$	$k=9$	$k=10$	$k=11$	$k=12$
$n=0$	$\frac{3}{2}$												
$n=2$	$\frac{3}{2}$	$-\frac{5}{2}$	$\frac{25}{12}$										
$n=4$	$\frac{3}{2}$	$-\frac{5}{4}$	$\frac{7}{12}$	$-\frac{9}{4}$	$\frac{49}{20}$								
$n=6$	$\frac{3}{2}$	$-\frac{31}{30}$	$\frac{7}{12}$	$-\frac{19}{20}$	$\frac{11}{30}$	$-\frac{13}{6}$	$\frac{761}{280}$						
$n=8$	$\frac{3}{2}$	$-\frac{20}{21}$	$\frac{7}{12}$	$-\frac{99}{140}$	$\frac{11}{30}$	$-\frac{143}{168}$	$\frac{15}{56}$	$-\frac{17}{8}$	$\frac{7381}{2520}$				
$n=10$	$\frac{3}{2}$	$-\frac{115}{126}$	$\frac{7}{12}$	$-\frac{171}{280}$	$\frac{11}{30}$	$-\frac{377}{630}$	$\frac{15}{56}$	$-\frac{289}{360}$	$\frac{19}{90}$	$-\frac{21}{10}$	$\frac{86021}{27720}$		
$n=12$	$\frac{3}{2}$	$-\frac{235}{264}$	$\frac{7}{12}$	$-\frac{101}{180}$	$\frac{11}{30}$	$-\frac{52}{105}$	$\frac{15}{56}$	$-\frac{2159}{3960}$	$\frac{19}{90}$	$-\frac{511}{660}$	$\frac{23}{132}$	$-\frac{25}{12}$	$\frac{1171733}{360360}$

APPENDIX B: THE NLO SPECTRAL DENSITY

The coefficients G_n^k and H_n^k in the expansion of the NLO perturbative spectral density (30) are collected in Tables IV and V, respectively. Our results for G_n^k agree with Ref. [14] (except for G_0^0 and G_4^0), noting an overall sign difference in definition of G_n^k, whereas for H_n^k the difference is that the expansion in Eq. (30) also involves contributions with odd $k = 2\ell + 1$.

[1] V. L. Chernyak and A. R. Zhitnitsky, JETP Lett. **25**, 510 (1977); Sov. J. Nucl. Phys. **31**, 544 (1980); V. L. Chernyak, A. R. Zhitnitsky, and V. G. Serbo, JETP Lett. **26**, 594 (1977); Sov. J. Nucl. Phys. **31**, 552 (1980).

[2] A. V. Radyushkin, Joint Institute for Nuclear Research Report No. R2-10717, 1977; [arXiv:hep-ph/0410276]; A. V. Efremov and A. V. Radyushkin, Theor. Math. Phys. **42**, 97 (1980); Phys. Lett. **94B**, 245 (1980).

[3] G. P. Lepage and S. J. Brodsky, Phys. Lett. **87B**, 359 (1979); Phys. Rev. D **22**, 2157 (1980).

[4] A. V. Efremov and A. V. Radyushkin, Joint Institute for Nuclear Research, Dubna Report No. JINR-E2-80-521, 1980.

[5] N. Isgur and C. H. Llewellyn Smith, Nucl. Phys. **B317**, 526 (1989); Phys. Lett. B **217**, 535 (1989).

[6] A. V. Radyushkin, Nucl. Phys. **A532**, 141 (1991).

[7] H. J. Behrend *et al.* (CELLO Collaboration), Z. Phys. C **49**, 401 (1991).

[8] J. Gronberg *et al.* (CLEO Collaboration), Phys. Rev. D **57**, 33 (1998).

[9] B. Aubert *et al.* (*BABAR* Collaboration), Phys. Rev. D **74**, 012002 (2006).

[10] B. Aubert *et al.* (The *BABAR* Collaboration), Phys. Rev. D **80**, 052002 (2009).

[11] A. V. Radyushkin, Phys. Rev. D **80**, 094009 (2009).

[12] M. V. Polyakov, JETP Lett. **90**, 228 (2009).

[13] A. E. Dorokhov, arXiv:1003.4693.

[14] S. V. Mikhailov and N. G. Stefanis, Nucl. Phys. **B821**, 291 (2009).

[15] S. V. Mikhailov, A. V. Pimikov, and N. G. Stefanis, arXiv:1010.4711.

[16] S. V. Mikhailov, A. V. Pimikov, and N. G. Stefanis, Phys. Rev. D **82**, 054020 (2010).

[17] A. Khodjamirian, Eur. Phys. J. C **6**, 477 (1999).

[18] A. Schmedding and O. I. Yakovlev, Phys. Rev. D **62**, 116002 (2000).

[19] A. P. Bakulev, S. V. Mikhailov, and N. G. Stefanis, Phys. Lett. B **508**, 279 (2001); **590**, 309(E) (2004).

[20] A. P. Bakulev, S. V. Mikhailov, and N. G. Stefanis, Phys. Rev. D **67**, 074012 (2003).

[21] A. P. Bakulev, S. V. Mikhailov, and N. G. Stefanis, Phys. Lett. B **578**, 91 (2004).

[22] S. S. Agaev, Phys. Rev. D **72**, 114020 (2005); **73**, 059902 (E) (2006)].

[23] I. V. Musatov and A. V. Radyushkin, Phys. Rev. D **56**, 2713 (1997).

[24] F. del Aguila and M. K. Chase, Nucl. Phys. **B193**, 517 (1981).

[25] E. Braaten, Phys. Rev. D **28**, 524 (1983).

[26] E. P. Kadantseva, S. V. Mikhailov, and A. V. Radyushkin, Yad. Fiz. **44**, 507 (1986) [Sov. J. Nucl. Phys. **44**, 326 (1986)].

[27] F. M. Dittes and A. V. Radyushkin, Phys. Lett. B **134**, 359 (1984).

[28] M. H. Sarmadi, Phys. Lett. B **143**, 471 (1984).

[29] G. R. Katz, Phys. Rev. D **31**, 652 (1985).

[30] S. V. Mikhailov and A. V. Radyushkin, Nucl. Phys. **B254**, 89 (1985).

[31] D. Müller, Phys. Rev. D **49**, 2525 (1994).

[32] D. Müller, Phys. Rev. D **51**, 3855 (1995).

[33] B. Melic, D. Müller, and K. Passek-Kumericki, Phys. Rev. D **68**, 014013 (2003).

[34] V. Braun and D. Müller, Eur. Phys. J. C **55**, 349 (2008).

[35] V. L. Chernyak and A. R. Zhitnitsky, Nucl. Phys. **B201**, 492 (1982); **B214(E)**, 547 (1983).

[36] V. L. Chernyak and A. R. Zhitnitsky, Phys. Rep. **112**, 173 (1984).

[37] A. Khodjamirian, T. Mannel, and M. Melcher, Phys. Rev. D **70**, 094002 (2004).

[38] P. Ball, V. M. Braun, and A. Lenz, J. High Energy Phys. 05 (2006) 004.
[39] S. V. Mikhailov and A. V. Radyushkin, Phys. Rev. D **45**, 1754 (1992).
[40] A. P. Bakulev and S. V. Mikhailov, Phys. Lett. B **436**, 351 (1998).
[41] A. P. Bakulev, S. V. Mikhailov, and N. G. Stefanis, Phys. Rev. D **73**, 056002 (2006).
[42] V. M. Braun, A. Khodjamirian, and M. Maul, Phys. Rev. D **61**, 073004 (2000).
[43] J. Bijnens and A. Khodjamirian, Eur. Phys. J. C **26**, 67 (2002).
[44] S. S. Agaev, Phys. Rev. D **72**, 074020 (2005).
[45] P. Ball and R. Zwicky, Phys. Lett. B **625**, 225 (2005).
[46] G. Duplancic, A. Khodjamirian, T. Mannel, B. Melic, and N. Offen, J. High Energy Phys. 04 (2008) 014; A. Khodjamirian, T. Mannel, N. Offen, and Y. M. Wang (work in progress).
[47] V. M. Braun *et al.*, Phys. Rev. D **74**, 074501 (2006).
[48] D. Antonio *et al.*, Proc. Sci., LAT2007 (2007) 329 [arXiv:0710.0869]; R. Arthur *et al.*, arXiv:1011.5906.
[49] I. I. Balitsky, V. M. Braun, and A. V. Kolesnichenko, Nucl. Phys. **B312**, 509 (1989).
[50] V. M. Braun and I. E. Filyanov, Z. Phys. C **44**, 157 (1989).
[51] V. L. Chernyak and I. R. Zhitnitsky, Nucl. Phys. **B345**, 137 (1990).
[52] M. A. Shifman, A. I. Vainshtein, and V. I. Zakharov, Nucl. Phys. **B147**, 385 (1979); , , and , **B147**, 448 (1979).
[53] V. Braun, P. Gornicki, and L. Mankiewicz, Phys. Rev. D **51**, 6036 (1995).
[54] A. Ali, V. M. Braun, and H. Simma, Z. Phys. C **63**, 437 (1994).
[55] P. Ball, V. M. Braun, and N. Kivel, Nucl. Phys. **B649**, 263 (2003).
[56] V. M. Belyaev, V. M. Braun, A. Khodjamirian, and R. Ruckl, Phys. Rev. D **51**, 6177 (1995).
[57] A. Khodjamirian, R. Ruckl, S. Weinzierl, and O. I. Yakovlev, Phys. Lett. B **457**, 245 (1999).
[58] T. M. Aliev and M. Savci, Phys. Rev. D **61**, 016008 (1999).
[59] T. M. Aliev, A. Ozpineci, S. B. Yakovlev, and V. Zamiralov, Phys. Rev. D **74**, 116001 (2006).
[60] T. M. Aliev, K. Azizi, A. Ozpineci, and M. Savci, Phys. Rev. D **80**, 096003 (2009).
[61] V. M. Braun and I. E. Filyanov, Z. Phys. C **48**, 239 (1990).
[62] P. Ball, J. High Energy Phys. 01 (1999) 010.
[63] V. A. Novikov *et al.*, Nucl. Phys. **B237**, 525 (1984).
[64] B. L. Ioffe and A. V. Smilga, Nucl. Phys. **B232**, 109 (1984).
[65] V. M. Belyaev and Y. I. Kogan, Yad. Fiz. **40**, 1035 (1984).
[66] I. I. Balitsky, A. V. Kolesnichenko, and A. V. Yung, Sov. J. Nucl. Phys. **41**, 178 (1985).
[67] I. I. Balitsky and V. M. Braun, Nucl. Phys. **B311**, 541 (1989).
[68] P. Ball and V. M. Braun, Phys. Rev. D **55**, 5561 (1997)
[69] S. J. Brodsky and G. F. de Teramond, Phys. Rev. D **77**, 056007 (2008).
[70] H. R. Grigoryan and A. V. Radyushkin, Phys. Rev. D **77**, 115024 (2008); A. Radyushkin, Int. J. Mod. Phys. A **25**, 502 (2010).
[71] V. M. Braun, E. Gardi, and S. Gottwald, Nucl. Phys. **B685**, 171 (2004).
[72] V. M. Braun and I. Halperin, Phys. Lett. B **328**, 457 (1994).
[73] S. S. Agaev and M. A. Gomshi Nobary, Phys. Rev. D **77**, 074014 (2008).
[74] C. J. Bebek *et al.*, Phys. Rev. D **17**, 1693 (1978).
[75] V. Tadevosyan *et al.*, Phys. Rev. C **75**, 055205 (2007); T. Horn *et al.*, Phys. Rev. Lett. **97**, 192001 (2006).
[76] C. Bourrely, I. Caprini, and L. Lellouch, Phys. Rev. D **79**, 013008 (2009).
[77] P. Ball and R. Zwicky, Phys. Rev. D **71**, 014015 (2005).
[78] P. del Amo Sanchez *et al.* (The *BABAR* Collaboration), arXiv:1010.0987.
[79] FEYNCALC: Tools and Tables for Quantum Field Theory Calculations, http://www.feyncalc.org/.
[80] P. Kroll, arXiv:1012.3542.